THE JOURNAL OF BIOLOGICAL CHEMISTRY VOL. 290, NO. 6, pp. 3248–3268, February 6, 2015
Published in the U.S.A.

Structural and Kinetic Basis of Steroid 17α,20-Lyase Activity in Teleost Fish Cytochrome P450 17A1 and Its Absence in Cytochrome P450 17A2*

Received for publication, November 19, 2014, and in revised form, December 16, 2014 Published, JBC Papers in Press, December 22, 2014, DOI 10.1074/jbc.M114.627265

Pradeep S. Pallan[‡], Leslie D. Nagy[‡], Li Lei[‡], Eric Gonzalez[‡], Valerie M. Kramlinger[‡], Caleigh M. Azumaya[‡], Zdzislaw Wawrzak[§], Michael R. Waterman[‡], F. Peter Guengerich[‡1], and Martin Egli[‡2]

From the [‡]Department of Biochemistry, Vanderbilt University School of Medicine, Nashville, Tennessee 37232 and the [§]Life Sciences Collaborative Access Team, Sector 21, Advanced Photon Source, Argonne National Laboratory, Argonne, Illinois 60439

Background: Fish (and human) P450 17A1 catalyze both steroid 17α-hydroxylation and 17α,20-lyase reactions. A second fish P450, 17A2 (51% identical), catalyzes only 17α-hydroxylation.
Results: Crystal structures of zebrafish P450 17A1 and 17A2 and human P450 17A1 are very similar.
Conclusion: In kinetic analysis, the two-step oxidation of progesterone is more distributive than for pregnenolone.
Significance: Small structural differences are associated with activities of the two fish P450s.

Cytochrome P450 (P450) 17A enzymes play a critical role in the oxidation of the steroids progesterone (Prog) and pregnenolone (Preg) to glucocorticoids and androgens. In mammals, a single enzyme, P450 17A1, catalyzes both 17α-hydroxylation and a subsequent 17α,20-lyase reaction with both Prog and Preg. Teleost fish contain two 17A P450s; zebrafish P450 17A1 catalyzes both 17α-hydroxylation and lyase reactions with Prog and Preg, and P450 17A2 is more efficient in pregnenolone 17α-hydroxylation but does not catalyze the lyase reaction, even in the presence of cytochrome b_5. P450 17A2 binds all substrates and products, although more loosely than P450 17A1. Pulse-chase and kinetic spectral experiments and modeling established that the two-step P450 17A1 Prog oxidation is more distributive than the Preg reaction, *i.e.* 17α-OH product dissociates more prior to the lyase step. The drug orteronel selectively blocked the lyase reaction of P450 17A1 but only in the case of Prog. X-ray crystal structures of zebrafish P450 17A1 and 17A2 were obtained with the ligand abiraterone and with Prog for P450 17A2. Comparison of the two fish P450 17A-abiraterone structures with human P450 17A1 (DeVore, N. M., and Scott, E. E. (2013) *Nature* 482, 116–119) showed only a few differences near the active site, despite only ~50% identity among the three proteins. The P450 17A2 structure differed in four residues near the heme periphery. These residues may allow the proposed alternative ferric peroxide mechanism for the lyase reaction, or residues removed from the active site may allow conformations that lead to the lyase activity.

Cytochrome P450 (P450)[3] enzymes are important in the metabolism of many exogenous and endogenous compounds, including steroids (1, 2). Of the 57 human P450s, at least 14 have important roles in steroid metabolism (2–4). One of these steroid-oxidizing enzymes is P450 17A1, which catalyzes the two-step oxidations of progesterone and pregnenolone (Fig. 1). At least 50 different variants of this enzyme have been identified in clinical settings (5). The enzyme is also a target for prostate cancer therapy, with at least two major drugs (abiraterone and orterenol (TAK-700) (6, 7)) in clinical use or development (Fig. 1).

Crystal structures of human P450 17A1 have been published with the inhibitor abiraterone bound (5) and, more recently, with the steroid substrates (8). However, the biochemical basis of the second oxidation step remains enigmatic. The second step, *i.e.* 17α,20-lyase or "desmolase" reaction (Fig. 1), has been proposed to involve a different form of reactive oxygen than that normally used in P450 reactions (FeO^{3+}), namely a ferric peroxide ($Fe^{(III)}O_2^-$) (9–11). Only the second step (lyase reaction) is stimulated by cytochrome b_5 (b_5), at least in mammalian systems, and the first step (17α-hydroxylation) is not (12, 13). Phosphorylation has been reported to have the same effect (14–16). Some humans have mutations that affect only the 17α,20-lyase reaction (2, 5), and one drug (orteronel (6)) has been developed that preferentially inhibits the second reaction in human P450 17A1 (7). b_5 stimulates the lyase reaction without transferring electrons (17), and NMR studies have provided evidence that both the NADPH-P450 reductase and b_5 share (and compete for) the same binding site on human P450 17A1 (18).

One issue with P450 17A1 is the processivity of the two reactions (Fig. 1). In multistep enzyme reactions, a processive reaction is one in which the intermediate products do not dissociate from the enzyme, as opposed to a distributive reaction in which they do dissociate and reassociate prior to further catalysis.

* This work was supported, in whole or in part, by National Institutes of Health Grants R01 GM103937, T32 ES007028, and P30 ES000267 (to M. E. and F. P. G.).
The atomic coordinates and structure factors (codes 4R1Z, 4R20, and 4R21) have been deposited in the Protein Data Bank (http://wwpdb.org/).

[1] To whom correspondence may be addressed: Dept. of Biochemistry, Vanderbilt University School of Medicine, 638 Robinson Research Bldg., 2200 Pierce Ave., Nashville, TN 37232-0146. Tel.: 615-322-2261; Fax: 615-343-0704; E-mail: f.guengerich@vanderbilt.edu.
[2] To whom correspondence may be addressed: Dept. of Biochemistry, Vanderbilt University School of Medicine, 868A Robinson Research Bldg., 2200 Pierce Ave., Nashville, TN 37232-0146. Tel.: 615-343-8070; Fax: 615-322-7122; E-mail: martin.egli@vanderbilt.edu.

[3] The abbreviations used are: P450, cytochrome P450; b_5, cytochrome b_5; DHEA, dehydroepiandrosterone; OH, hydroxy; SAD, single wavelength anomalous dispersion; TAK-700, orteronel; ID, insertion device; r.m.s.d., root mean square deviation.

With the bovine enzyme, Yamazaki *et al.* (19) concluded that the system was distributive, although more processive with the pregnenolone reaction. Others have concluded that the enzyme is either distributive (20) or rather processive (19, 21–26), with some of the results depending on the animal model.

Some of the details of P450 17A1 reactions vary among animal species (27). In teleost fish, two P450 17A enzymes are present, one (17A1) that catalyzes both the 17α-hydroxylation and 17α,20-lyase reactions and one (17A2) that only catalyzes the former (28). A biological reason for the existence of the two enzymes in fish is not clear, and the molecular basis for the absence of the lyase activity in P450 17A2 has not been examined.

The existence of the two closely related fish P450 17A1 enzymes differing in the lyase step presents an opportunity to identify the basis of the 17α,20-lyase activity, not only in the P450 17A1 enzymes in fish but also other species. We purified these enzymes and characterized their binding and catalytic behavior with their substrates progesterone and pregnenolone. The processivity of zebrafish P450 17A1 was analyzed. We also compared x-ray crystal structures of zebrafish P450s 17A1 and 17A2, as well as with human P450 17A1, and we noted several minor structural differences that may be critical in understanding the basis of lyase function.

EXPERIMENTAL PROCEDURES

Chemicals and Reagents—Progesterone (Sigma), 17α-OH progesterone, androstenedione (Steraloids, Newport, RI), pregnenolone (Sigma), 17α-OH pregnenolone (Steraloids), and DHEA (Steraloids) were obtained from the indicated sources. Abiraterone was purchased from Selleckchem (Houston, TX). Orteronel (TAK-700) was a generous gift of Millennium Pharmaceuticals (Cambridge, MA).

Enzymes—Escherichia coli recombinant rat NADPH-P450 reductase was prepared as described (29). Some preliminary results with b_5 were obtained using *E. coli* recombinant human b_5 (30, 31).

Zebrafish P450 17A1 and P450 17A2 Cloning, Expression, and Purification—In the zebrafish *CYP17A1* open reading frame, the region encoding the N-terminal transmembrane helix (residues 1–26) was replaced by DNA coding for MAKKTSSKGK (P450 2C3 N-terminal region (32)), and the 3′ end was extended by 18 nucleotides encoding six histidines. A V57R mutation was introduced to generate a trypsin cleavage site to increase the solubility of the protein. The entire modified cDNA was synthesized by GenScript (Piscataway, NJ) and inserted into a pET17b expression vector (EMD Millipore, Billerica, MA).

The *CYP17A2* cDNA from zebrafish was cloned as follows. RNA was extracted from fresh zebrafish ovaries, and the cDNA was amplified by RT-PCR (Qiagen One Step RT-PCR kit). The region encoding the N-terminal transmembrane helix (residues 1–25) was replaced by DNA coding for MAKKTSSKGK (P450 2C3 N-terminal region (32)); the 3′ end was extended by 18 nucleotides encoding six histidines, and the modified cDNA was inserted into a pET17B vector (EMD Millipore).

Zebrafish P450 17A1 and 17A2 expression and purification for enzymatic experiments were as follows: the P450 plasmids and a pGro12 (ES/EL) expression vector (33) were transformed into *E. coli* BL21-Gold (DE3) competent cells. A single colony of bacteria was used to inoculate Luria-Bertani (LB) media containing ampicillin (100 μg/ml) and kanamycin (50 μg/ml) for an overnight culture incubated at 37 °C and shaking at 250 rpm (Multifors Incubator) for 12–14 h. One-liter expression cultures were initiated by diluting the overnight culture 100-fold into Terrific Broth (TB) media containing 100 μg/ml ampicillin, 50 μg/ml kanamycin, and 250 μl of trace elements mixture (34). The expression culture was incubated at 37 °C, 250 rpm, until the OD_{600} reached ~1.0. The expression culture was then supplemented with 1.0 mM isopropyl β-D-1-thiogalactopyranoside, 1.0 mM δ-aminolevulinic acid, and 27 mM arabinose and incubated at 28 °C, 120 rpm for ~40 h. Typical expression levels of zebrafish P450 17A1 and 17A2 (determined spectrally (35)) were 500 and 1100 nmol of P450/liter of culture, respectively.

Cultures were harvested by centrifugation at $2.5 \times 10^3 \times g$ and 4 °C for 30 min. All purification steps were done at 0–4 °C. The bacterial pellet from each 1 liter of expression culture was then suspended in 300 ml of 0.10 M Tris-HCl buffer (pH 7.6) containing 0.5 mM EDTA and 0.5 M sucrose, and 60 μl of lysozyme solution (50 mg/ml) was added per g of bacterial pellet. The bacterial suspension was mixed with gentle swirling and incubated on ice for 30 min, with additional swirling every 10 min. The suspensions were then centrifuged at $2.5 \times 10^3 \times g$ for 30 min. The resulting spheroplast pellets were then suspended in 0.10 M potassium phosphate buffer (pH 7.6) containing 20% glycerol (v/v), 6 mM $Mg(CH_3CO_2)_2$, 0.1 mM dithiothreitol, and a protease inhibitor mixture (Complete Tablets, EDTA-free, EASYpack, Roche Applied Science)). The suspension was then supplemented with 1 μl of 0.1 M phenylmethylsulfonyl fluoride (PMSF, in cold acetone) per ml of suspension, and the cells were lysed by sonication. Unbroken cells and debris were eliminated with $10^4 \times g$ centrifugation for 20 min. The supernatant was then centrifuged at $1.4 \times 10^5 \times g$ for 60 min to sediment the bacterial membranes. The membrane pellets were then suspended in 0.10 M potassium phosphate buffer (pH 7.6) containing 20% glycerol (v/v), 0.1 mM dithiothreitol, and 1% sodium CHAPS (w/v) using a Dounce homogenizer and stirred gently overnight. The solubilized proteins were then separated from the membranes by centrifugation (60 min) at $1.4 \times 10^5 \times g$. The supernatant, containing the solubilized membrane proteins, was then supplemented with 0.5 M NaCl and 20 mM imidazole and loaded onto a (1.5 cm × 8.5 cm) Ni^{2+}-nitrilotriacetic acid column pre-equilibrated with 10 bed volumes of the same buffer (containing 1% CHAPS (w/v) and 20 mM imidazole). After loading, the bound proteins were washed with 10 bed volumes of the same buffer and eluted with the same buffer containing 200 mM imidazole. The eluted P450 fractions (based on A_{417} measurements) were pooled and dialyzed three times against 100 volumes of 0.20 M potassium phosphate buffer (pH 7.6) containing 20% glycerol (v/v), 0.1 mM EDTA, and 0.1 mM dithiothreitol, aliquoted, and stored at −80 °C.

For x-ray crystallographic experiments, zebrafish P450 17A1 and 17A2 were expressed and purified as described previously for *E. coli* recombinant bovine P450 21A2 (36), including Ni^{2+}-nitrilotriacetate, DEAE, and SP-Sepharose chromatography steps. The proteins were each eluted from an SP-Sepharose Fast Flow

FPLC column (GE Healthcare) with 50 mM potassium phosphate buffer (pH 7.4) containing 20% glycerol (v/v), 0.1 mM dithiothreitol, 0.1 mM EDTA, 0.004% (w/v) 3,6,9,12,15,18,21,24,27-nonaoxanonatriacontan-1-ol (C12E9) detergent (Anatrace, Maumee, OH), and either 500 mM NaCl (for P450 17A1) or 250 mM NaCl (for P450 17A2). Purified zCYP17s were obtained in yields between 300 and 600 nmol/liter culture.

b_5 Cloning, Expression, and Purification—Zebrafish b_5 (69% identical to human microsomal b_5) was cloned from an embryo cDNA library (5 days post-fertilization), obtained as a gift from Prof. R. D. Cone, Vanderbilt University. The b_5 cDNA was amplified using the 5′ oligonucleotide GGAGGAATAAACCATGGCAAACAACGGTACAGACGG (to add an NcoI restriction site) and the 3′ oligonucleotide CAGCCAAGCTTCTATCATTATCATGCCTCCTCTGCAGTG (to add two additional stop codons and a HindIII restriction site). The b_5 pre-expression construct was then obtained from ligation of the amplified cDNA to a pSE420 vector (Invitrogen), using the specified restriction sites. Sequencing results revealed three base differences, T27G, C75T, and T117C, when compared with the coding sequence specified in the reported mRNA sequence (NM_213135). Only the first of these differences, resulting in an N9K amino acid substitution, was corrected by site-directed mutagenesis in the final b_5 expression construct.

A single colony of *E. coli* JM109 competent cells, transformed with the zebrafish b_5 expression construct, was used to inoculate LB media containing 100 μg/ml ampicillin for a 16-h overnight pre-culture (incubated at 37 °C, with shaking at 250 rpm in a Multifors incubator). The expression culture consisted of a 100-fold dilution of pre-culture into 1 liter of TB media containing 1 mM NaCl, 2 g of Bactopeptone (Difco), 100 μg/ml ampicillin, 340 mg of thiamine, and 250 μl of a trace elements solution (34). The expression culture was incubated at 37 °C (250 rpm in Multifors incubator until its OD_{600} reached ~0.75). Expression was then induced by supplementing the culture to 1.0 mM isopropyl β-D-1-thiogalactopyranoside and 1.0 mM δ-aminolevulinic acid, changing the incubation conditions to 30 °C (at 200 rpm in the same incubator), and continuing for ~48 h.

The cultures were harvested by centrifugation at $2.5 \times 10^3 \times g$ and 4 °C for 30 min. All purification steps were done at 0–4 °C. A bacterial pellet from 1 liter of expression culture was then suspended in 300 ml of 0.10 M Tris-Cl buffer (pH 7.6) containing 0.5 mM EDTA and 0.5 M sucrose, and 60 μl of a solution of 50 mg/ml lysozyme was added per g of bacterial pellet. The bacterial suspension was mixed with gentle swirling and incubated on ice for 30 min, with additional swirling every 10 min. The suspensions were then centrifuged at $2.5 \times 10^3 \times g$ for 30 min. The resulting spheroplast pellets were suspended in 20 mM potassium phosphate buffer (pH 7.6) containing 20% glycerol (v/v), 0.1 mM EDTA, and a protease inhibitor mixture (Complete Tablets EDTA-free, EASYpack, Roche Applied Science). The suspension was then supplemented with 1 μl of 0.1 M PMSF (in cold acetone) per ml of suspension, and the cells were lysed by sonication. Unbroken cells and debris were eliminated with a $10^4 \times g$ centrifugation for 20 min. The supernatant was then centrifuged at $1.4 \times 10^5 \times g$ for 60 min to separate the soluble fraction from the bacterial membranes. (The b_5 remaining in the membrane pellet was solubilized with detergent (cholate) and purified, but subsequent work showed that it was inhibitory, in contrast to the stimulation seen with soluble b_5.)

Sodium cholate (0.5%, w/v) was added to the soluble fraction, and the resulting clarified solution was loaded onto a DE-Sephacel column (2.5 × 25 cm) pre-equilibrated with 7 bed volumes of 20 mM potassium phosphate buffer (pH 7.6) containing 20% glycerol (v/v), 0.1 mM EDTA, and 0.5% sodium cholate (w/v). After loading, the bound proteins were first washed with 20 bed volumes of the same buffer, followed by 20 bed volumes of 20 mM potassium phosphate buffer (pH 7.6) containing 20% glycerol (v/v), 0.1 mM EDTA, 0.5% sodium cholate (w/v), and 0.10 M NaCl. The bound proteins were eluted with a linear gradient composed of 400 ml of the latter buffer (0.10 M NaCl) and 400 ml of the same buffer containing 0.4 M NaCl. The fractions eluted in a peak at ~0.3 M NaCl (based on A_{413} measurements) were pooled and dialyzed twice against 50 volumes of 20 mM potassium phosphate buffer (pH 7.6) containing 20% glycerol (v/v) and 0.1 mM EDTA, aliquoted, and stored at −20 °C. The final amount of recovered protein was 515 nmol from a 6-liter culture, based on spectral quantitation (37).

Preparation of P450 Complexes for Crystallization—To generate complexes, inhibitor (abiraterone, in $(CH_3)_2SO$) or substrate (progesterone, in C_2H_5OH (P450 17A2)) was added to purified protein. The protein to arbiraterone molar ratio was 1:10 and the P450 17A2 to progesterone molar ratio was 1:2. The complexes were concentrated to 30 mg of protein/ml in 50 mM potassium phosphate buffer (pH 7.4) containing 10% glycerol (v/v), 0.1 mM dithiothreitol, 1 mM EDTA, 0.004% C12E9 detergent (w/v), and either 125 mM NaCl (P450 17A1) or 40 mM NaCl (P450 17A2).

Crystallization and in Situ Proteolysis of the P450 17A1·Abiraterone Complex—Prior to setting up crystallization droplets, subtilisin was added to the complex (30 mg/ml protein concentration) such that the protease to P450 17A1 ratio (w/w) was 1:1000. Ten μl of this mixture was removed and incubated at room temperature for 30 min for N-terminal sequence analysis (see below). Crystals were grown using the sitting-drop vapor diffusion technique by mixing equal volumes of complex solution and mother liquor (0.1 M imidazole (pH 6.5) and 1.0 M sodium acetate) and equilibrating droplets against 60 μl of reservoir solution at 20 °C. Crystals of the P450 17A1 complex with abiraterone appeared within a few days. One round of microseeding was performed to optimize the size of crystals. Wells containing microcrystals were washed with 10 μl of reservoir buffer, and the mixture was then transferred to a microcentrifuge tube with 40 μl of mother liquor and a PTFE Seed Bead (Hampton Research, Aliso Viejo, CA). After mixing the contents of the tube with a vortex device and diluting 1:1000 with mother liquor (v/v), 200 nl of the solution was mixed with 200 nl of protein for each drop. Larger crystals of the complex (with typical sizes of 0.2–0.25 mm) grew from micro-seeded droplets. Crystals were mounted in nylon loops and swiped through a droplet of 30% (v/v) glycerol in mother liquor prior to flash freezing in liquid nitrogen.

Crystallization and in Situ Proteolysis of P450 17A2·Progesterone Complex—Prior to setting up crystallization droplets, trypsin was added to the complex (30 mg of protein/ml)

such that the protease to P450 17A2 ratio (w/w) was 1:1000. Ten μl of this mixture was removed and incubated at room temperature for 30 min for N-terminal sequence analysis (see below). Crystals of the P450 17A2 complex with progesterone were grown by the sitting drop-vapor diffusion technique by mixing equal volumes (200 nl) of complex solution and mother liquor (100 mM sodium HEPES buffer (pH 7.5), 50 mM $MgCl_2$, and 30% (v/v) polyethylene glycol monomethyl ether 3550) and equilibrating droplets against 60 μl of reservoir solution at 20 °C. Crystals appeared after several days and were cryoprotected by soaking them in mother liquor with 15% glycerol (v/v) prior to mounting in nylon loops and flash freezing in liquid nitrogen.

Crystallization and in Situ Proteolysis of the P450 17A2·Abiraterone Complex—In situ proteolysis was done as in the case of the progesterone complex. Crystals of the abiraterone complex were grown by mixing equal volumes (200 nl) of complex solution and mother liquor (1% (w/v) tryptone, 50 mM sodium HEPES (pH 7.0), and 20% (w/v) polyethylene glycol 3350) and equilibrating droplets against 60 μl of reservoir solution at 20 °C. Crystals appeared after several days and were soaked in 5 mM CH_3HgCl prior to cryoprotecting and flash freezing them in the same fashion as described above for the progesterone complex.

N-terminal Sequence Analysis of P450 17A1 and P450 17A2 Proteins after Protease Treatment—Digested samples were analyzed on a 10% SDS gel (w/v) and transferred to a polyvinylidene fluoride (PVDF) membrane, and the target bands (40–50 kDa) were cut out and submitted for N-terminal sequence analysis (Jodie Franklin, Synthesis and Sequence Facility, The Johns Hopkins University, Baltimore, MD). In the case of complexes treated with trypsin, Edman degradation showed that the N-terminal residue of P450 17A2 in the crystals was Ser-52, consistent with trypsin cleaving exclusively C-terminal to arginine (Arg-51 in the case of zebrafish P450 17A2) or lysine residues (38), and in accord with the first residue visible in the electron density maps being Leu-54.

The outcome of the Edman degradation analysis was less conclusive in the case of the treatment of P450 17A1 with subtilisin. SDS-PAGE of protein treated with the protease indicated a mixture of products. Edman degradation placed the N terminus at Gly-37. The protein in the crystal had the first residue visible in electron density maps at Ser-83.

X-ray Diffraction Data Collection and Processing—All data were collected on insertion device (ID) beam lines of the Life Sciences Collaborative Access Team (LS-CAT), located at Sector 21 of the Advanced Photon Source, Argonne National Laboratory (Argonne, IL). Data for crystals of the P450 17A2 complex with abiraterone soaked in 5 mM CH_3HgCl were collected on Sector 21-ID-D at a wavelength of 1.0039 Å and a Mar300 CCD detector. Data for crystals of the P450 17A1 complex with abiraterone were also collected on Sector 21-ID-D but at a wavelength of 1.7341 Å to exploit the anomalous signal of iron. Data for crystals of the P450 17A2 complex with progesterone were collected on Sector 21-ID-F, at a wavelength of 0.9787 Å and a Mar225 CCD detector. Data were processed with the program HKL2000 (39) or, alternatively, with xia2/XDS (40) and Pointless/Aimless (40, 41). Selected crystal data and data collection statistics are summarized (Table 4, see below).

Phasing, Model Building, and Refinement—The structures of the P450 17A1 and 17A2 abiraterone complexes were solved by single-wavelength anomalous dispersion (SAD). The program phenix.autosol in the PHENIX software package (42) was used to locate and refine the positions of substructures (iron with P450 17A1 and mercury with P450 17A2), calculate the initial phases, and carry out density modification and model building with auto-build. The automatically built initial models were carefully examined inside the experimental electron density maps, and extensive manual building was subsequently performed with the program Coot (43). Both structures were refined with the program Refmac 5 (44) in the CCP4 suite (45). The structure of the P450 17A2·progesterone complex was subsequently determined by molecular replacement with the program PHASER (46), using the complex of P450 17A2 with abiraterone as the search model. As in the case of the P450 17A2·abiraterone complexes, the program Refmac 5 (44) was used for refining the structure of P450 17A2 in complex with progesterone.

Estimation of Dissociation Constants for Ligand Binding—In general, P450 (1–2 μM) was used in 100 mM potassium phosphate buffer (pH 7.4). Two 1-ml glass cuvettes (1.0 cm path length) were placed in an Aminco DW2a-OLIS spectrophotometer (On-Line Instrument Systems, Bogart, GA), and the baseline was balanced electronically (23 °C). Varying aliquots of each potential ligand (dissolved in C_2H_5OH, 0.5 μl per aliquot) were added to the sample cuvette, and the same volume of solvent was added to the reference cuvette. The contents of each cuvette were mixed using a plumping device (Semi-microcuvette Add-a-mixer, type P68, NSG Precision Cells, Farmingdale, NY), and spectra were recorded. Plots of $\Delta(A_{390} - A_{420})$ *versus* [ligand] were fit (hyperbolae, single-site equation) using GraphPad Prism software (GraphPad, La Jolla, CA).

In cases with initial apparent K_d values of < 2 μM, the titrations were repeated using a 10-cm path length cylindrical cuvette (Starna Cells, Atascadero, CA, catalogue no. 34-Q-100, volume 25 ml) in a Cary 14/OLIS spectrophotometer (On-Line Instrument Systems). The sample (100 nM P450, in 100 mM potassium phosphate buffer (pH 7.4), was used to record a baseline, and additions were made to the cuvette, recording spectra each time. Plots of $\Delta(A_{max} - A_{min})$ were fit (in GraphPad Prism) to quadratic Equation 1,

$$Y = B + (A/2) \cdot (1/E) \cdot ((K_d + E + X) - \text{sqrt}((K_d + E + X)\text{^}2 - (4 \cdot E \cdot X))) \quad \text{(Eq. 1)}$$

Assays of Catalytic Activity—In general, incubations (at 37 °C) were done in 100-μl volumes and included 0.5 μM P450, 1.0 μM NADPH-P450 reductase, 10 μg ml^{-1} L-α-1,2-dilauroyl-*sn*-glycero-3-phosphocholine, 100 mM potassium phosphate buffer (pH 7.4), varying concentrations of progesterone or pregnenolone (dissolved in C_2H_5OH), and (added to start reactions) an NADPH-regenerating system consisting of (final concentrations) 10 mM glucose 6-phosphate, 0.5 mM $NADP^+$, and 1 IU/ml yeast glucose-6-phosphate dehydrogenase (47).

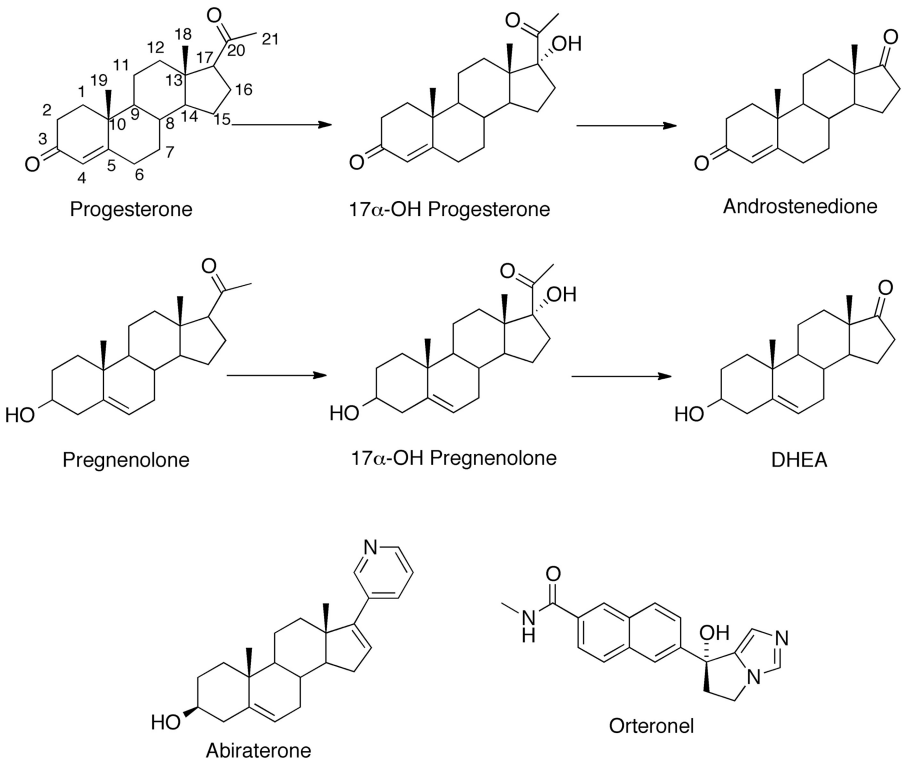

FIGURE 1. **Reactions catalyzed by P450 17A enzymes and structures of inhibitors.**

When radioactive assays were done, either [4-^{14}C]progesterone, [7-^{3}H]pregnenolone, or 17α-[1,2,6,7-^{3}H]OH progesterone was used as the substrate. In assays for conversion of progesterone to 17α-OH progesterone and androstenedione, reactions were stopped by the addition of 50 μl of CH_3CN and mixed, and 50 μl (⅓ of total) was applied to the loading zone of a 20 × 20-cm, 250-μm channeled analytical TLC plate (Silica Gel G, Analtech, Newark, DE). The samples were dried (~30 min) using the draft in the door of a fume hood, and the plates were developed in a solvent system consisting of ethyl acetate/CH_2Cl_2 (1:4, v/v). Standards of 17α-OH progesterone and androstenedione, added to some of the lanes, were used to locate the products in the samples, using 254-nm UV light. The zones were marked, and the appropriate sections were scraped into 7-ml vials for liquid scintillation counting. CH_3OH (0.5 ml) was added to each vial, followed by brief shaking to elute steroids. Scintillation mixture (5 ml of Scintiverse, Fisher) was added to each vial, followed by dark adaptation overnight (to eliminate luminescence artifacts) and counting in a Beckman LS6500 instrument (4 min). In some cases, radioactivity on the TLC plates was scanned with an AR-2000 Radio-TLC Imaging Scanner (Bioscan, Poway, CA) (instead of scraping and liquid scintillation counting).

In the case of (unlabeled) pregnenolone, reactions were quenched by the addition of 1.0 ml of CH_2Cl_2. The products were extracted by mixing with a vortex device, followed by centrifugation (2 × 10^3 × *g*, 10 min) and transfer of 0.8 ml of the organic phase to new tubes. The solvent was removed under a nitrogen stream, and the samples were dissolved in 150 μl of 50 mM potassium phosphate buffer (pH 7.4). *Streptomyces* sp. cholesterol oxidase (Sigma, 2 units/sample) was added, and the reaction proceeded for 2 h, converting 17α-OH pregnenolone to 17α-OH progesterone and DHEA to androstenedione. These products were separated by TLC and counted as described for the progesterone assays.

Radioactive 17α-OH pregnenolone was not commercially available as substrate, and reactions were done with unlabeled material. The reactions proceeded as described for the radioactive assays, and the product DHEA was converted to androstenedione with cholesterol oxidase (see above). Analysis of the resulting androstenedione was done with a Waters Acquity UPLC BEH octadecylsilane (C_{18}) column (2.1 × 100 mm, 1.7 μm) in a Waters Acquity UPLC system. LC conditions were as follows: solvent A contained 70% CH_3OH and 30% H_2O (v/v), and solvent B was 100% CH_3CN. The following gradient program was used with a flow rate of 0.3 ml min^{-1}: 0–2 min, hold at 10% B (v/v), 2–4 min, linear gradient from 10% B to 25% B (v/v); 4–4.5 min, hold at 25% B, 4.5–5 min, linear gradient from 25% B to 10% B (v/v); 5–7 min hold at 10% B. The temperature of the column was maintained at 40 °C.

Pulse-Chase and Pulse-Chase Kinetic Assays—These experiments were set up using the same procedure as described for TLC assays for the conversion of [4-^{14}C]progesterone to androstenedione and [7-^{3}H]pregnenolone to DHEA (TLC assays) (see above). After each reaction was initiated, varying concentrations of unlabeled 17α-hydroxyprogesterone or 17α-hydroxypregnenolone (5–80 μM) were added (after 60 s) to the incubations, which then continued for 11 min (at 37 °C). Radiolabeled androstenedione and DHEA were measured in the respective experiments in which these products were formed (Fig. 1).

Pulse-chase kinetic assays were conducted as described above; however, in addition, aliquots at various time points after the chase (30, 60, 120, 300, and 660 s) were collected and analyzed.

Stopped-flow Kinetics—An OLIS RSM-1000 instrument (On-Line Instrument Systems) was used in the rapid-scanning mode, with 1.24-mm slits and a 20-mm path length, at 23 °C. One syringe contained 4 μM zebrafish P450 17A1 in 100 mM potassium phosphate buffer (pH 7.4) and 120 μM L-α-1,2-dilauroyl-*sn*-glycero-3-phosphocholine, plus (when indicated) 4 μM 17α-OH progesterone or 17α-OH pregnenolone. The other syringe contained 20 μM orteronel (TAK-700) in 100 mM potassium phosphate buffer, with 120 μM L-α-1,2-dilauroyl-*sn*-glycero-3-phosphocholine. Equations 2 and 3 were used,

$$\text{P450} \cdot 17\alpha\text{-OH steroid} \underset{k_{-1}}{\overset{k_1}{\rightleftharpoons}} \text{P450} + 17\alpha\text{-OH steroid}$$

$$\lambda_{max}\ 390\ \text{nm} \quad \text{(Eq. 2)}$$

and

$$\text{P450} + \text{orteronel} \underset{k_{-2}}{\overset{k_2}{\rightleftharpoons}} \text{P450} \cdot \text{orteronel}$$

$$\lambda_{max}\ 434\ \text{nm} \quad \text{(Eq. 3)}$$

and the changes in A_{392} and A_{434} were used to estimate rates. The singular value decomposition mode of the OLIS software was used (two-state system, with background), either with the complete wavelength range (370–520 nm) or, in some cases, the 370–420 nm data set. Means ± S.D. of at least five separate experiments are presented. Orteronel was used as a trapping reagent, and the rates of back-reactions (k_{-1} and k_{-2}) were ignored. The apparent rate of k_2 was measured at 7.7 (± 0.4) s^{-1} with 10 μM orteronel at 23 °C. Thus, measurement of the rate of conversion of a P450 17A1·17α-OH steroid complex to a P450 17A1·orteronel complex is an estimate of k_1 (Equations 1 and 2).

Kinetic Analysis—K_d, k_{cat}, and K_m values were estimated from hyperbolic fits in GraphPad Prism, with quadratic analysis for tight-binding situations (see above). IC_{50} values were fit in the same program using the formula: Y = bottom + (top − bottom)/(1 + 10^(X − logIC_{50})).

Pulse-chase results were fit to a kinetic model designed to analyze the extent of processivity. KinTek Explorer® software was employed for global fitting of the pulse-chase experimental data (48). The fitting was constrained in part by assuming diffusion-limited binding of progesterone, pregnenolone, androstenedione, and DHEA and by using measured dissociation constants (K_d) and dissociation rates (k_{off}) for 17α·OH progesterone or 17α·OH pregnenolone complexes.

RESULTS

Purification of Zebrafish Proteins—The expression of P450s 17A1 and 17A2 and b_5 from zebrafish cDNA clones was relatively straightforward. The P450s were prepared with C-terminal His_5 tags; b_5 was expressed without a tag and, under the conditions used here, was recovered in the supernatant fraction following centrifugation at $10^5 \times g$. The b_5 was readily purified by ion-exchange chromatography. Electrophoretic and spectral data are presented in Fig. 2, and the yields are given under "Experimental Procedures."

Preliminary Assays of Product Formation and the Effect of b_5—Zebrafish P450 17A1 converted progesterone to 17α-OH progesterone and androstenedione and converted pregnenolone to 17α-OH pregnenolone and DHEA, as reported for the recombinant tilapia enzyme expressed in human embryonic kidney cells (Fig. 3) (28). In both cases, the temporal patterns were indicative of sequential oxidation (Fig. 3, *A* and *B*). With both progesterone and pregnenolone, the accumulation of the 17α-OH steroid was less, and the final product was more pronounced in the presence of b_5 (Fig. 3, *A* and *B*). Similar patterns were observed with human and zebrafish b_5 (results not shown). The extent of b_5 stimulation (≤2-fold) was much less than found for human P450 17A1 (13).

Zhou *et al.* (28) reported that recombinant tilapia P450 17A2 did not have 17α,20-lyase activity with progesterone or pregnenolone (in human embryonic kidney cells). We found the same results with zebrafish P450 17A2, even with purified zebrafish b_5 present and continuing for extended times. With both P450 17A2 and pregnenolone (Fig. 3*D*), the reaction appeared to stop after ~60% of the substrate was consumed. HPLC searches for further products (UV, MS, and ^{14}C) did not reveal any further oxidation of 17α-OH pregnenolone.

Estimation of Steady-state Kinetic Parameters and Binding Constants—The preliminary time course studies indicated that P450 17A2 was more active than P450 17A1 in the 17α-hydroxylation of both progesterone and pregnenolone (Fig. 3). Steady-state kinetic parameters for oxidations were measured, using early time points to minimize the lyase reactions of P450 17A1 (Table 1). The lyase reactions were measured using the 17α-OH steroids as substrates.

P450 17A1 had 3-fold higher catalytic efficiency in the 17α-hydroxylation of progesterone than pregnenolone (Table 1). P450 17A1 appeared to be a better catalyst of the progesterone 17α,20-lyase reaction than the pregnenolone 17α,20-lyase reaction. Both P450s had similar progesterone 17α-hydroxylation activity and, despite having high K_m values, P450 17A2 was a more efficient catalyst of pregnenolone 17α-hydroxylation than P450 17A1.

K_d values were measured for binding of the steroid substrates and products to P450 17A1 and 17A2 (Fig. 4 and Table 2). As outlined under "Experimental Procedures," in many cases P450s change the iron spin state upon substrate binding, due to displacement of H_2O as the distal ligand (to the heme iron). A direct contact is not made between the iron and the atoms of the substrate. A nitrogenous "type II" ligand (orteronel in this case) can bind directly to the iron, involving the formation of an Fe···N bond and giving a different Soret spectrum. In the cases of high affinity, the concentration of P450 was lowered 10-fold by performing the titrations in a 10-cm path length cell, and analysis was done with a quadratic equation. Several of the results are of interest. (i) The affinity of P450 17A2 for all steroids was lower than for P450 17A1. (ii) The affinity of 17α-OH pregnenolone was higher than pregnenolone or DHEA for both P450 17A1 and 17A2, a point that is considered later regarding

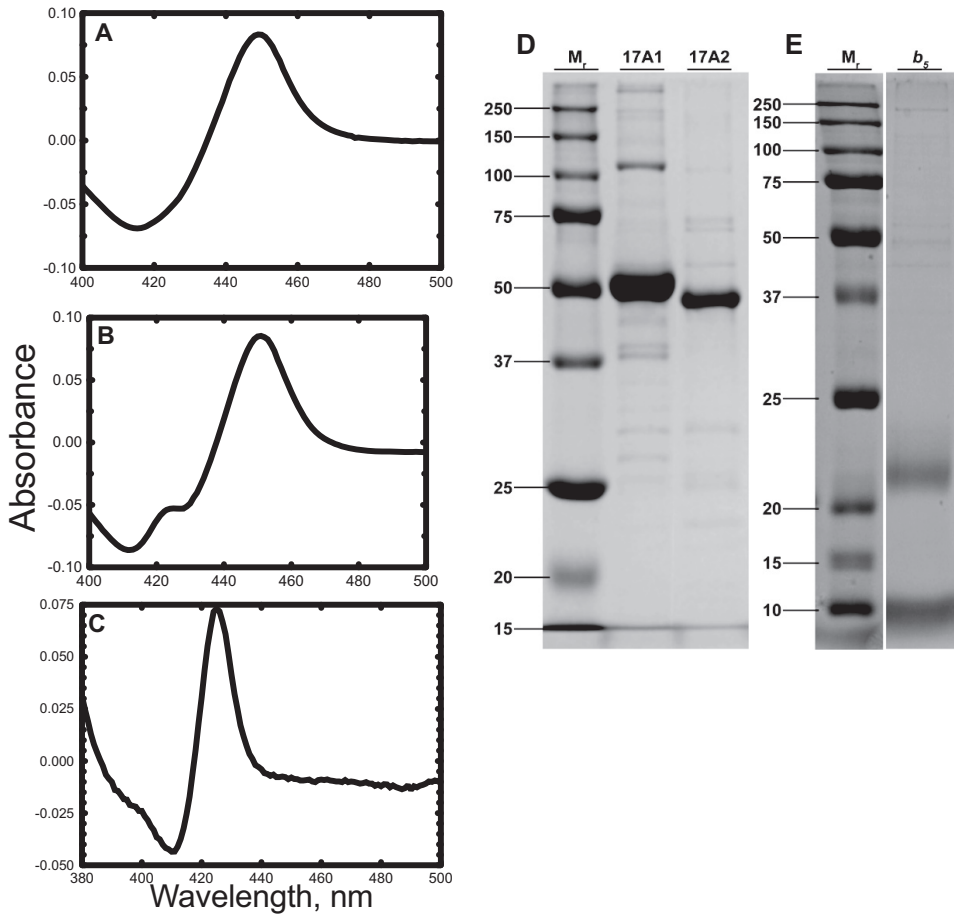

FIGURE 2. **Spectra and gel electrophoresis of purified recombinant zebrafish hemoproteins.** *A*, P450 17A1; *B*, P450 17A2; *C*, b_5. The concentrations were 0.93, 1.03, and 0.63 μM, respectively. The P450 spectra (*A* and *B*) were Fe^{2+}·CO *versus* Fe^{2+} difference spectra (both λ_{max} 450 nm) (35), and the b_5 spectrum was an Fe^{2+} *versus* Fe^{3+} spectrum (λ_{max} 424 nm) (37). *D*, SDS-PAGE of P450s 17A1 (apparent M_r 51,500) and 17A2 (apparent M_r 54,000); *E*, SDS-PAGE of b_5 (apparent M_r 21,000). (Bands at the bottom of the gel are due to the dye front.) M_r standards are shown in the labeled lanes.

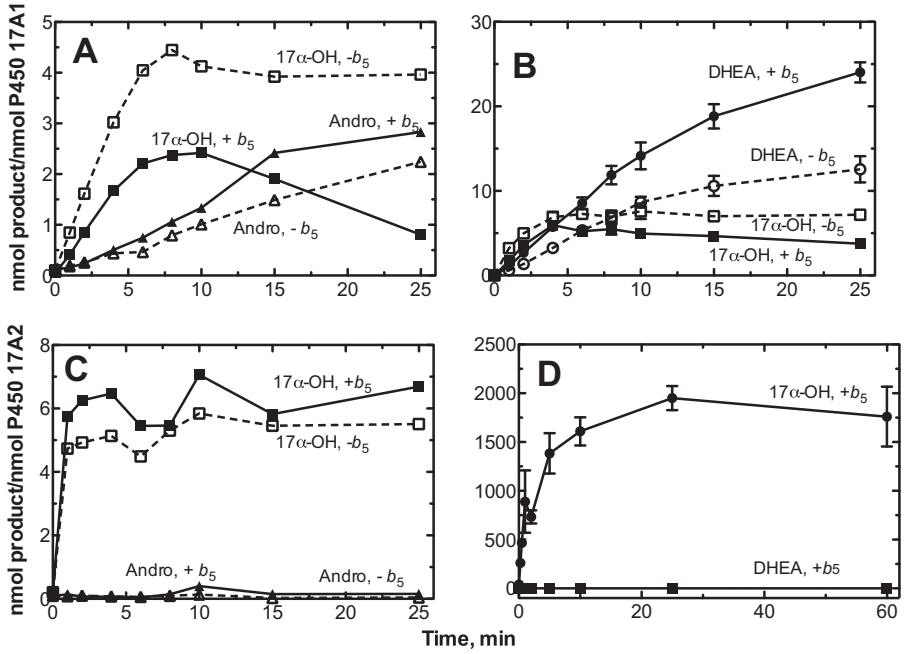

FIGURE 3. **Time courses of steroid oxidations by P450 17A1 and 17A2 in the absence (*open symbols*) and presence (*closed symbols*) of b_5.** *A*, progesterone oxidation by P450 17A1. □ and ■, 17α-OH progesterone (*17α-OH*); △ and ▲, androstenedione (*Andro*). *B*, pregnenolone; ○ and ●, DHEA. *C*, progesterone oxidation by P450 17A2. □ and ■, 17α-OH progesterone (*17α-OH*); △ and ▲, androstenedione. *D*, pregnenolone oxidation by P450 17A2. ●, 17α-OH pregnenolone (*17α-OH*); ■, DHEA.

TABLE 1
Steady-state kinetic parameters for oxidation of steroids by zebrafish P450 17A enzymes

Reaction	P450 17A1			P450 17A2		
	k_{cat}	K_m	k_{cat}/K_m	k_{cat}	K_m	k_{cat}/K_m
	min^{-1}	μM	$\mu M^{-1}\ min^{-1}$	min^{-1}	μM	$\mu M^{-1}\ min^{-1}$
Progesterone → 17α-OH	5.8 ± 0.6	1.7 ± 0.9	3.4 ± 1.8	95 ± 9	30 ± 7	3.2 ± 0.8
17α−OH Progesterone → androstenedione	1.2 ± 0.1	1.1 ± 0.3	1.1 ± 0.3	[a]	[a]	[a]
Pregnenolone → 17α-OH	2.0 ± 0.2	2.0 ± 0.4	1.0 ± 0.2	51 ± 2	9.3 ± 0.8	5.5 ± 0.5
Pregnenolone 17αOH → DHEA	0.33 ± 0.01	8.5 ± 0.7	0.039 ± 0.004	[a]	[a]	[a]

[a] No product was detected (Fig. 2).

processivity. (iii) The K_d values appear to bear limited relation to the K_m values or the catalytic efficiencies in Table 1.

In other titrations, both abiraterone and orteronel (see below) yielded type II spectral changes, due to the binding of nitrogenous ligands (pyridine and imidazole) to ferric iron (5). The K_d values for abiraterone, estimated spectrally, were 17 ± 6 nM for P450 17A1 and 120 ± 50 nM for P450 17A2 (data not presented). The K_d values for orteronel were 30 ± 8 nM for P450 17A1 and 10 ± 24 nM for P450 17A2 (the error in the last value is high not because of data scatter but because the inherent difficulty in fitting such tight-binding data with the enzyme concentration in excess of the ligand).

Processivity of P450 17A1 Oxidations, Orteronel Inhibition—One of the outstanding questions about P450 17A enzymes is its processivity, *i.e.* the extent to which the 17α-OH product dissociates and rebinds before the 17α,20-lyase reaction (19–23, 26). The drug orteronel has been reported to preferentially inhibit the 17α,20-lyase reaction of human P450 17A1 (7), which is of practical value in the inhibition of androgen production without inhibiting the production of glucocorticoid steroids in castration-resistant prostate cancer (6). However, the selectivity of orteronel for the 17α-hydroxylation *versus* lyase reaction (Fig. 1) has been reported to vary in different animal species (7, 49). Accordingly, we measured IC_{50} values for the individual reaction with zebrafish P450 17A1 and 17A2 (Table 3). If a two-step reaction is totally processive, then one would not expect differential inhibition of the two steps, barring a totally allosteric effect (which is unlikely here in that the ligand is known to bind to the heme iron in the active site, see above).

Several interesting results were seen consistently (Table 3). Orteronel was a preferential inhibitor of the lyase reaction but only in the case of progesterone (with zebrafish P450 17A1). IC_{50} values were similar for both steps in the P450 17A1-catalyzed oxidation of pregnenolone. With P450 17A2 (which only does the 17α-hydroxylation step), orteronel was a much better inhibitor for progesterone 17α-hydroxylation than for the same reaction with pregnenolone. A simple explanation is that it is easier for orteronel to compete with progesterone (K_d 1.5 μM) than pregnenolone (K_d 0.36 μM) for the active site (for P450 17A1) (Table 2). The same logic follows for the 17α-OH compounds (Table 2), and the same pattern applies for P450 17A2.

Processivity of P450 17A1 Oxidation, Pulse-Chase Experiments—One of the most effective ways of addressing the issue of processivity in multistep reactions is with the use of pulse-chase experiments. P450 17A1 reactions were initiated with ^{14}C-labeled progesterone or pregnenolone for 1 min, and then unlabeled 17α-OH steroid was added; the reactions continued for another 11 min (Fig. 5). With progesterone, increasing amounts of unlabeled 17α-OH progesterone produced a gradual decrease in the amount of androstenedione formed (Fig. 5, *A* and *B*). However, with pregnenolone, only about one-half of the incorporation of label could be blocked with the maximum concentration of 17α-OH pregnenolone (Fig. 5, *C* and *D*). The addition of b_5 did not affect the pattern with either steroid (Fig. 5, *A versus B* and *C versus D*).

Estimation of P450 17A1 k_{off} Rates from 17α-OH Steroid Complexes—The spectral properties of complexes of P450 17A1 with steroids are very different from the complex with orteronel (Fig. 6, *A–C*). The low K_d values of P450 17A1·17α-OH steroid complexes allowed these to be prepared with a minimal concentration of free steroid (Table 2). Because the reaction of unbound P450 17A1 with orteronel is fast (measured at 7.7 (± 0.4) s^{-1} with 10 μM orteronel), the rate of dissociation of P450 17A1·17α-OH steroid complexes could be readily measured in orteronel trapping experiments (Fig. 6, *E–H*). The uncorrected k_{off} rate with 17α-OH progesterone was 1.56 (± 0.03) s^{-1} (94 min^{-1}, Fig. 6*E*) and with 17α-OH pregnenolone was 0.137 (± 0.012) s^{-1} (8.2 min^{-1}, Fig. 6*G*) (measured at 23 °C). When b_5 was present in the 17α-OH pregnenolone experiment, the k_{off} rate was 0.18 (± 0.05) s^{-1} (Fig. 6*H*).

Coupling the k_{off} rates with K_d values (Table 2 and Fig. 4) yielded k_{on} rates of ~10^7 M^{-1} s^{-1} (at 23 °C) for both 17α-OH progesterone and 17α-OH pregnenolone, which are typical for diffusion-limited reactions with enzymes (50). These k_{on} values were coupled with other K_d values (Table 2) to estimate k_{off} rates for the other P450 17A1·steroid complexes as follows: P450 17A1·progesterone (250 min^{-1}), P450 17A1·androstenedione (50 min^{-1}), P450 17A1·pregnenolone (220 min^{-1}), and P450 17 A1·DHEA (130 min^{-1}) (Fig. 7).

Kinetic Modeling of Pulse-Chase Data—The k_{cat} and k_{off} values were used as a starting point in a pulse-chase model involving the addition of 17α-OH steroids to P450 17A1 reactions initiated with radiolabeled progesterone or pregnenolone for 60 s. The program KinTek Explorer® (48) was used to derive rate constants and fit lines to the data sets (Fig. 8). Sets of rate constants were optimized to fit the data sets, and the optimized values are presented in Fig. 9. k_{on} rate constants of 10^7 M^{-1} s^{-1} (typical for diffusion-limited binding of substrates to enzymes) were consistent with K_d values and measured k_{off} rates (Figs. 6 and 7) and were used with the binding of substrate and products. The *k* values for the oxidation reactions are greater than the measured k_{cat} values, in that the k_{cat} parameter reflects the contributions of several steps. The fits show the lag for androstenedione production from progesterone (Fig. 8*A*) and a lack of a lag in the conversion of pregnenolone to DHEA (Fig. 8*B*), consistent with other experiments (Fig. 3, *A* and *B*) (note the

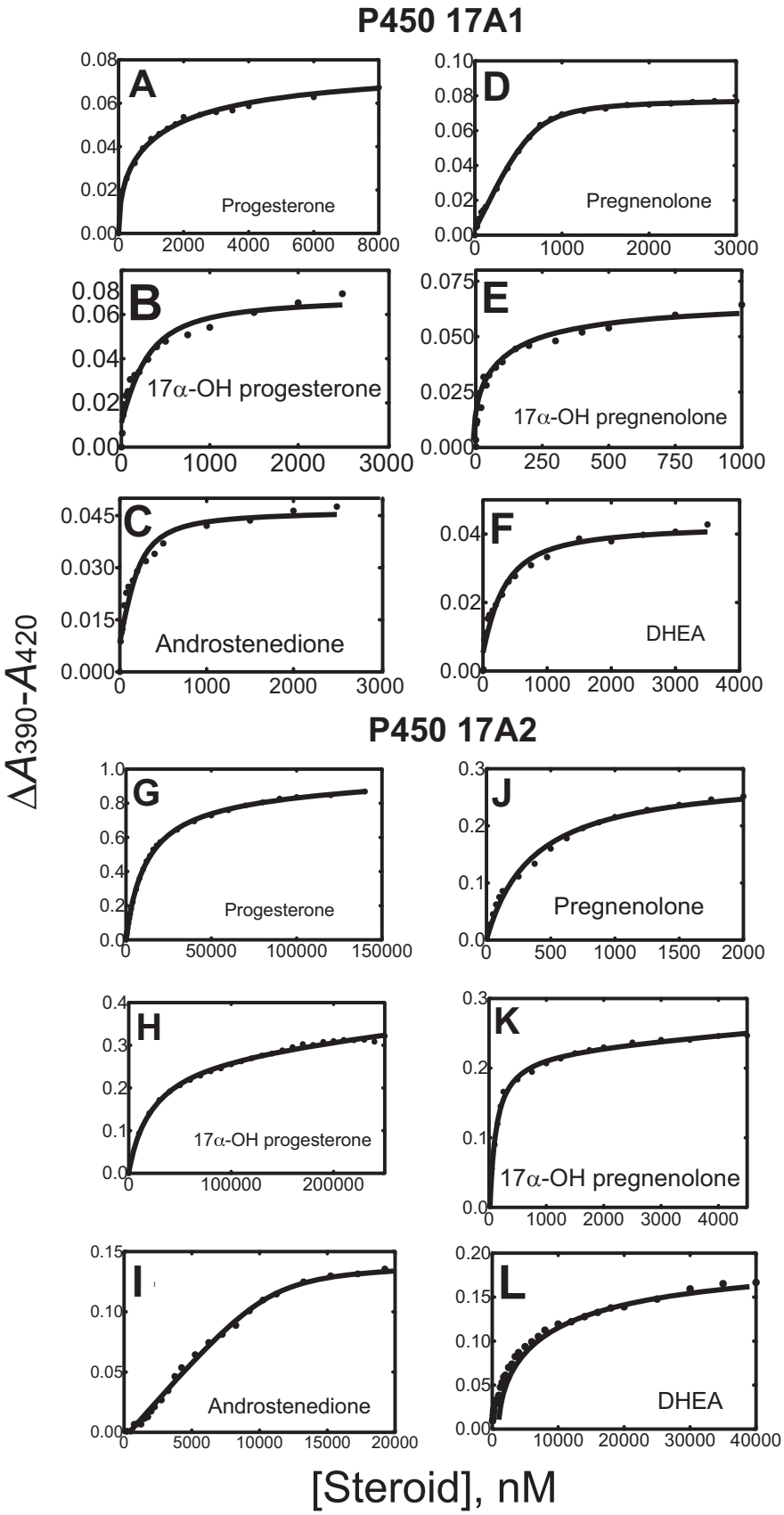

FIGURE 4. **Binding of steroids to zebrafish P450s 17A1 and 17A2.** The type I change of low-spin to high-spin iron was monitored in each case, with quadratic fitting of the data (ΔA_{390}–A_{420}) to a uni-molecular binding model (with quadratic equation for fitting, see under "Experimental Procedures"). See Table 2 for estimated K_d values. *A–F*, zebrafish P450 17A1. *A*, progesterone; *B*, 17α-OH progesterone; *C*, androstenedione; *D*, pregnenolone; *E*, 17α-OH pregnenolone; *F*, DHEA. *G–L*, zebrafish P450 17A2. *G*, progesterone; *H*, 17α-OH progesterone; *I*, androstenedione; *J*, pregnenolone; *K*, 17α-OH pregnenolone; *L*, DHEA.

TABLE 2
K_d values for steroids with P450 17A1 and 17A2

Steroid	K_d	
	P450 17A1	P450 17A2
	μM	
Progesterone	0.43 ± 0.04	13 ± 1
17α-OH Progesterone	0,17 ± 0.06	23 ± 2
Androstenedione	0.082 ± 0.035	13 ± 2
Pregnenolone	0.36 ± 0.03	0.36 ± 0.03
17α-OH Pregnenolone	0.014 ± 0.005	0.097 ± 0.019
DHEA	0.22 ± 0.06	2.5 ± 0.3

TABLE 3
IC_{50} values for inhibition of steroid oxidation by orteronel

Reaction	IC_{50}[a]	
	P450 17A1	P450 17A2
	nM	
Progesterone → 17α-OH	15 ± 1	1.1 ± 0.1
17α-Progesterone → androstenedione	0.14 ± 0.04	–[b]
Pregnenolone → 17α-OH pregnenolone	0.35 ± 0.34	790 ± 5
17α-OH pregnenolone → DHEA	0.17 ± 0.01	–[b]

[a] Means ± range of duplicate determinations are shown.
[b] No product was formed (see Fig. 2).

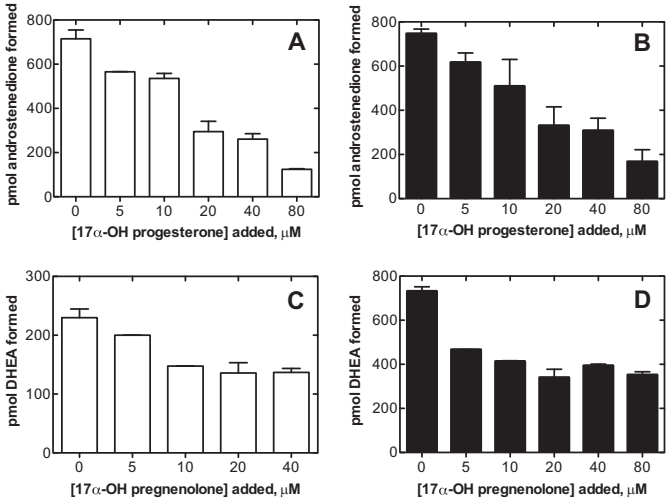

FIGURE 5. **Pulse-chase experiments with P450 17A1 and 17α-OH steroids.** In each case a P450 17A1 reaction was done with 0.5 μM P450 17A1, 1.0 μM NADPH-P450 reductase, 100 mM potassium phosphate, 15 μM L-α-1,2-dilauroyl-*sn*-glycero-3-phosphocholine, and either 50 μM [4-^{14}C]progesterone (10 μCi μmol^{-1}) or 50 μM [7-^{3}H]pregnenolone (10 mCi μmol^{-1}) at 37 °C. (The reactions began with the addition of an NADPH-generating system (47).) When indicated, b_5 (0.5 μM) was also present at the start. After 60 s, the indicated concentrations of 17α-OH progesterone or 17α-OH pregnenolone was added, and the reactions continued another 11 min at 37 °C. *A*, conversion of [^{14}C]progesterone to androstenedione without b_5. *B*, conversion of [^{14}C]progesterone to androstenedione, with b_5 present. *C*, conversion of [^{3}H]pregnenolone to DHEA, without b_5. *D*, conversion of [^{3}H]pregnenolone to DHEA, with b_5 present.

production of 4 pmol of DHEA in the 60-s incubation time before addition of 17α-OH pregnenolone in Fig. 8*B*).

Crystallization of the Zebrafish P450 17A1 Complex with Abiraterone and the P450 17A2 Complexes with Abiraterone and Progesterone—The zebrafish P450 17A1 and 17A2 proteins were expressed in their wild-type forms or with an alternative N-terminal leader sequence from P450 2C3 (MAKKTSSKGK) that replaced the N-terminal transmembrane helix (first 26 and 25 amino acids, respectively, see Fig. 10). All proteins were expressed with a C-terminal His_6 tag to facilitate purification by affinity chromatography. Although the proteins could be expressed in good yield and were highly pure and soluble, the crystals that grew were not of diffraction quality. Limited proteolysis *in situ* is a helpful approach to generate crystals of protein fragments in cases where full-length constructs resist crystallization (52, 53). To overcome the problems of crystal quality, we treated the P450 17A1 and 17A2 proteins with trypsin and α-chymotrypsin. Five mg of protein was mixed with 50, 5, 0.5, or 0.05 ng of protease, and the cleavage products were analyzed by SDS-PAGE. In the case of P450 17A2, the treatment with the highest amount of trypsin resulted in a major cleavage product that appeared as a band in the 50-kDa range. However, neither treatment with trypsin nor with α-chymotrypsin produced a viable P450 17A1 fragment; trypsin cleaved the protein virtually in the middle; and α-chymotrypsin, even at the higher concentrations, appeared unable to cleave the P450 17A1 protein to any significant extent. Because N-terminal sequence analysis indicated that trypsin cleavage of P450 17A2 had occurred at Arg-51, we mutated the corresponding residue in P450 17A1 (Val-57; Fig. 10) to arginine, in the hope of obtaining a major cleavage product of this protein as a result of treatment with trypsin. However, an SDS-PAGE assay demonstrated that the V57R mutant protein was not cleaved by the protease at this site. Next, we tested the Proti-Ace and Proti-Ace2 protease kits (Hampton Research) with P450 17A1. Both kits are composed of six different proteases, and the digest with subtilisin resulted in three major fragments, of which the first was slightly longer than the P450 17A2 fragment obtained with trypsin (Edman degradation showed that the N-terminal residue was Gly-37). A second fragment was somewhat shorter, and Ser-83 was the first residue visible in the electron density maps of the P450 17A1·abiraterone complex (Fig. 11). We subsequently used *in situ* proteolysis of P450 17A1 protein with subtilisin and P450 17A2 protein with trypsin to produce diffraction quality crystals of the complexes with the inhibitor abiraterone and with the substrate progesterone (P450 17A2; Table 4). Shortened constructs of the two proteins that were produced based on the proteolytic cleavage patterns of subtilisin (P450 17A1) and trypsin (P450 17A2) did not express well. Thus, it appears that the length of the N-terminal sequence is crucial for optimal expression levels with these P450 proteins and that *in situ* proteolysis is a useful approach for generating structural data for the zebrafish P450 17A1 and 17A2 protein complexes.

Crystal Structures of Zebrafish P450 17A1 and 17A2 in Complex with Abiraterone—The structures of the P450 17A1 and 17A2 proteins with the bound inhibitor abiraterone were both phased by SAD. We exploited the presence of Fe^{3+} coordinated to the porphyrin at the P450 active site to solve the structure of the P450 17A1 complex by Fe-SAD (Fig. 11). (The preparation of Figs. 11–16 and all superimpositions of structures were carried out with the program UCSF Chimera (54). Specifically, we used the matchmaker option employing the Needleman-Wunsch alignment algorithm and the matrix BLOSUM-62, along with default options for other parameters, *e.g.* residue and atom choice.) Crystals of the P450 17A2 complex were soaked in CH_3HgCl, and the structure was phased by Hg-SAD (Fig. 12). A summary of the crystal data, diffraction data collection, and refinement parameters is provided in Table 4. Both structures feature two independent complexes (termed A and B) per crystallographic asymmetric unit, whereas the P450 chains in mod-

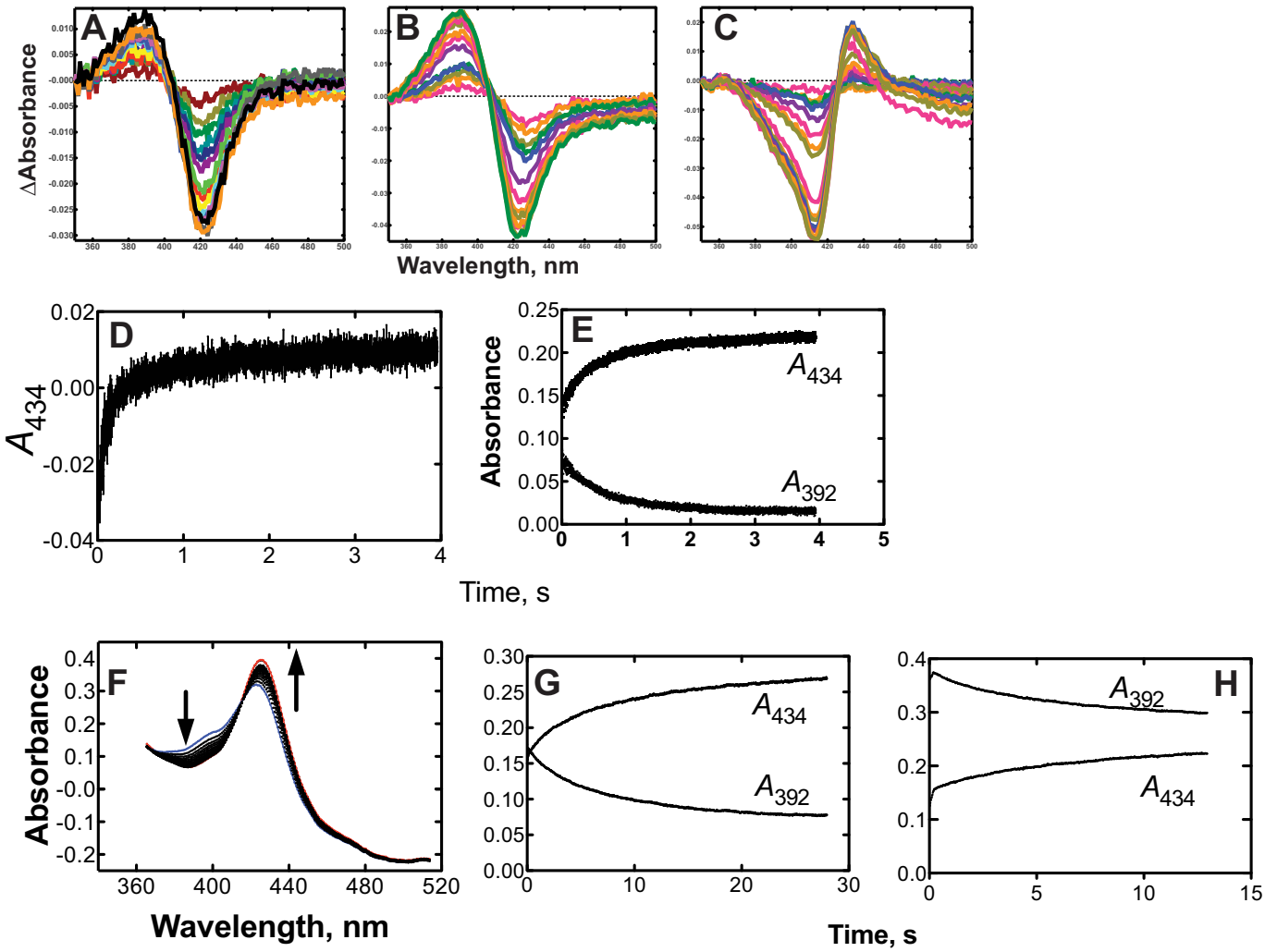

FIGURE 6. **Difference spectra of P450 17A1 with 17α-OH steroids and orteronel and estimation of rates of 17α-OH steroid dissociation from P450 17A1 using trapping with orteronel.** *A–C*, difference spectra from titrations of P450 17A1 with ligands (Table 2). *A*, 17α-OH progesterone; *B*, 17α-OH pregnenolone; *C*, orteronel. The highest concentration used (maximum change) was 10 μM for 17α-OH progesterone and 3 μM for 17α-OH pregnenolone and orteronel. *D*, kinetic trace of binding of 2 μM P450 17A1 with 10 μM orteronel. The estimated rate (k_{on}) was 7.7 ± 0.4 s^{-1}. *E*, kinetic trace of reaction of P450 17A1·17α-OH progesterone complex (2 μM) with 10 μM orteronel. The estimated rate was 1.56 ± 0.03 s^{-1}. *F*, 20 scans of the reaction of P450 17A1·17α-OH pregnenolone complex (2 μM) with 10 μM orteronel, collected over a period of 30 s. *G*, kinetic trace of reaction of P450 17A1·17α-OH pregnenolone complex (2 μM) with 10 μM orteronel. The estimated rate was 0.14 ± 0.01 s^{-1}. *H*, kinetic trace of reaction of P450 17A1·17α-OH pregnenolone complex (2 μM) with 10 μM orteronel in the presence of 2 μM b_5. The estimated rate was 0.18 ± 0.05 s^{-1}. *D–F*, and *H*, results are presented as means ± S.D. for ≥5 independent shots/traces.

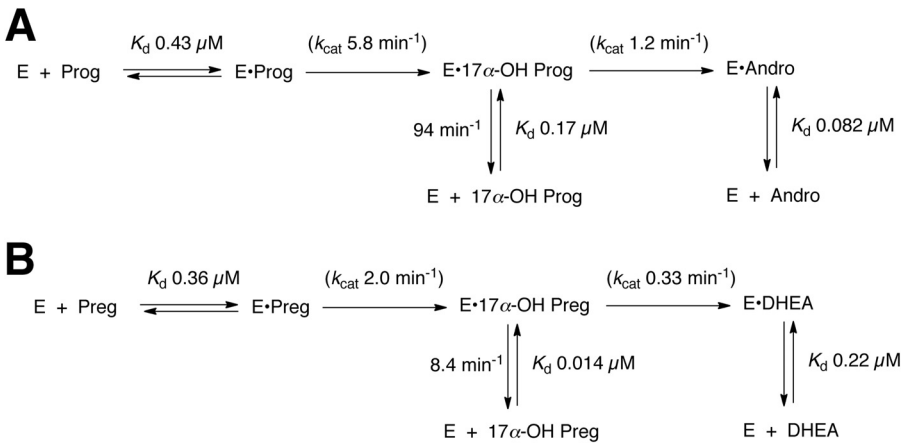

FIGURE 7. **Kinetics and binding parameters with zebrafish P450 17A1.** *A*, progesterone (*Prog*) oxidation; *B*, pregnenolone (*Preg*) oxidation. The k_{off} rates are from Fig. 5 and K_d values from Table 2. *Andro,* androstenedione.

els A and B of the P450 17A1 complex are composed of 411 and 405 amino acids, respectively. In the case of the P450 17A2 complex, the P450 chains of models A and B are composed of 423 and 425 amino acids, respectively. In addition to the missing 82 (P450 17A1) and 52 residues (P450 17A2) in the N-terminal region, residues absent in the crystallographic models map to various loop regions (Table 4, Figs. 11 and 12). However, despite the limited resolution of the structures (3.3 Å for P450 17A1 and 2.9 Å for P450 17A2; Table 4), the quality of the electron density is very good (Figs. 11*B* and 12*B*), and the protein, heme, and ligand atoms feature reasonable temperature factors. Complex models A and B in both structures display similar conformations as illustrated by superimpositions (Figs. 11*C* and 12*C*). As expected, loop regions on the surface show somewhat larger deviations than active site residues in the P450 core, the latter including heme and abiraterone.

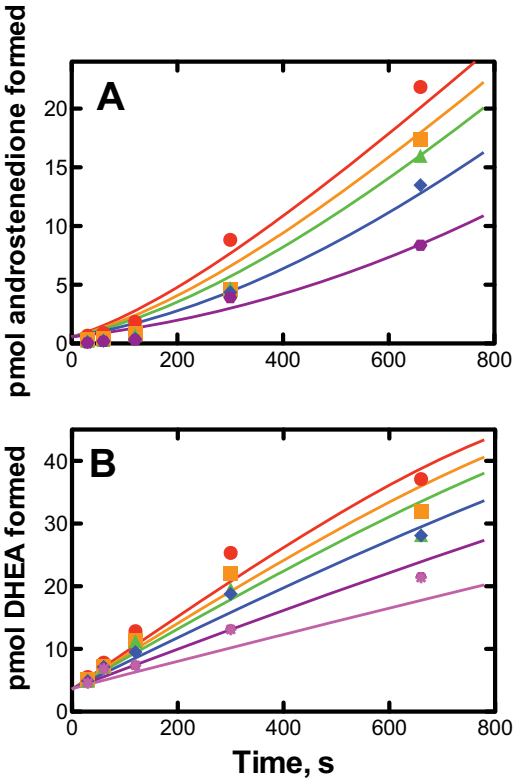

FIGURE 8. **Kinetics of zebrafish P450 17A1 catalysis under pulse-chase conditions.** *A*, androstenedione formation; *B*, DHEA formation. Concentrations of 17α-OH progesterone or 17α-OH pregnenolone used to chase the reaction were 0 (*red*), 5 (*orange*), 10 (*green*), 20 (*blue*), 40 (*purple*), and 80 μM (*pink*, for *B* only). Products were monitored in a reaction of P450 17A1 (0.5 μM) and [4-^{14}C]progesterone or [7-^{3}H]pregnenolone. Global fitting (using KinTek Explorer® software) is shown with the lines.

Crystal Structure of Zebrafish P450 17A2 in Complex with Progesterone—The structure of the complex between P450 17A2 and progesterone was determined by molecular replacement using the P450 17A2 protein portion from the abiraterone complex as the search model (Fig. 11). The crystal structures of the P450 17A2 abiraterone and progesterone complexes are isomorphous (Table 4). Although the resolution of the latter is somewhat higher (2.73 Å), the numbers of observed protein residues in the abiraterone and progesterone complex structures are very similar (848 *versus* 845, respectively). As in the case of the P450 17A1·abiraterone and 17A2·abiraterone complexes, the conformations adopted by the two independent P450 17A2 progesterone complexes per crystallographic asymmetric unit are very similar (Fig. 13*C*). A comparison of the positions of progesterone at the active site of P450 17A2 (Fig. 13*B*) and abiraterone at the active sites of P450 17A1 (Fig. 11*B*) and 17A2 (Fig. 12*B*) reveals the larger spacing between heme and substrate. The separation between Fe^{3+} and the nitrogen atom (N22) from the pyridine ring of abiraterone was 1.92 Å, on average. By comparison, the distance between C17 of progesterone and Fe^{3+} was 4.87 Å (average between molecules A and B). However, if we assume a perferryl state with a single oxygen wedged between iron and progesterone carbon (Fe^{4+}-O···C17), the Fe···C distance is reduced to ~3.7 Å and that between iron and H17(C17) to ~3 Å. At the opposite end of the substrate molecule, the hydroxyl group (O3) is too far removed to engage in an H-bond with Asn-209 (average distance between O3 and Cγ of Asn-209 5.9 Å), which protrudes from the ceiling of the active site (Fig. 13*B*). By comparison, the abiraterone molecule is somewhat longer, and in the structures of the P450 17A1 and 17A2 complexes with the inhibitor, the corresponding hydroxyl group forms an H-bond. In the P450 17A1 complex,

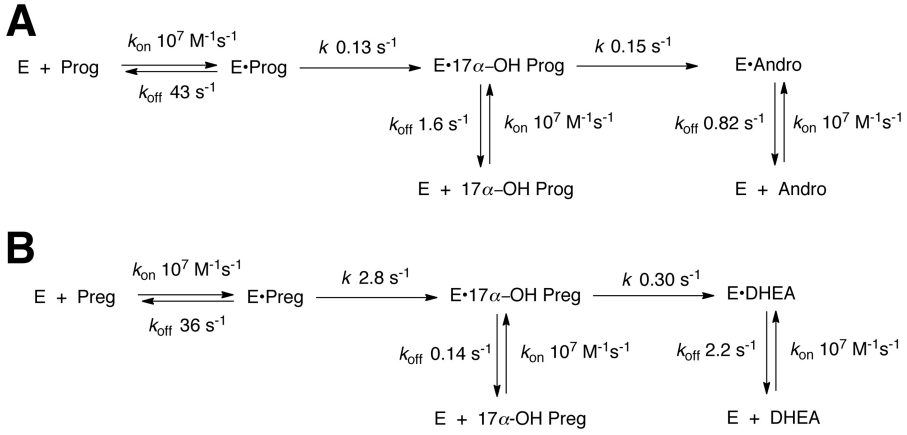

FIGURE 9. **Kinetics and binding parameters with zebrafish P450 17A1.** *A*, progesterone (*Prog*) oxidation; *B*, pregnenolone (*Preg*) oxidation. Rates for k_{on} were assumed to be diffusion-limited; k_{off} rates were calculated from measured K_d values (Table 2), and *k* values (rate constants) for catalytic steps were generated from global fitting of pulse-chase data (Fig. 7). Note that the units of time are seconds instead of minutes in this figure in light of the usual conventions, *e.g.* regarding typical diffusion-limited rate constants. *Andro*, androstenedione.

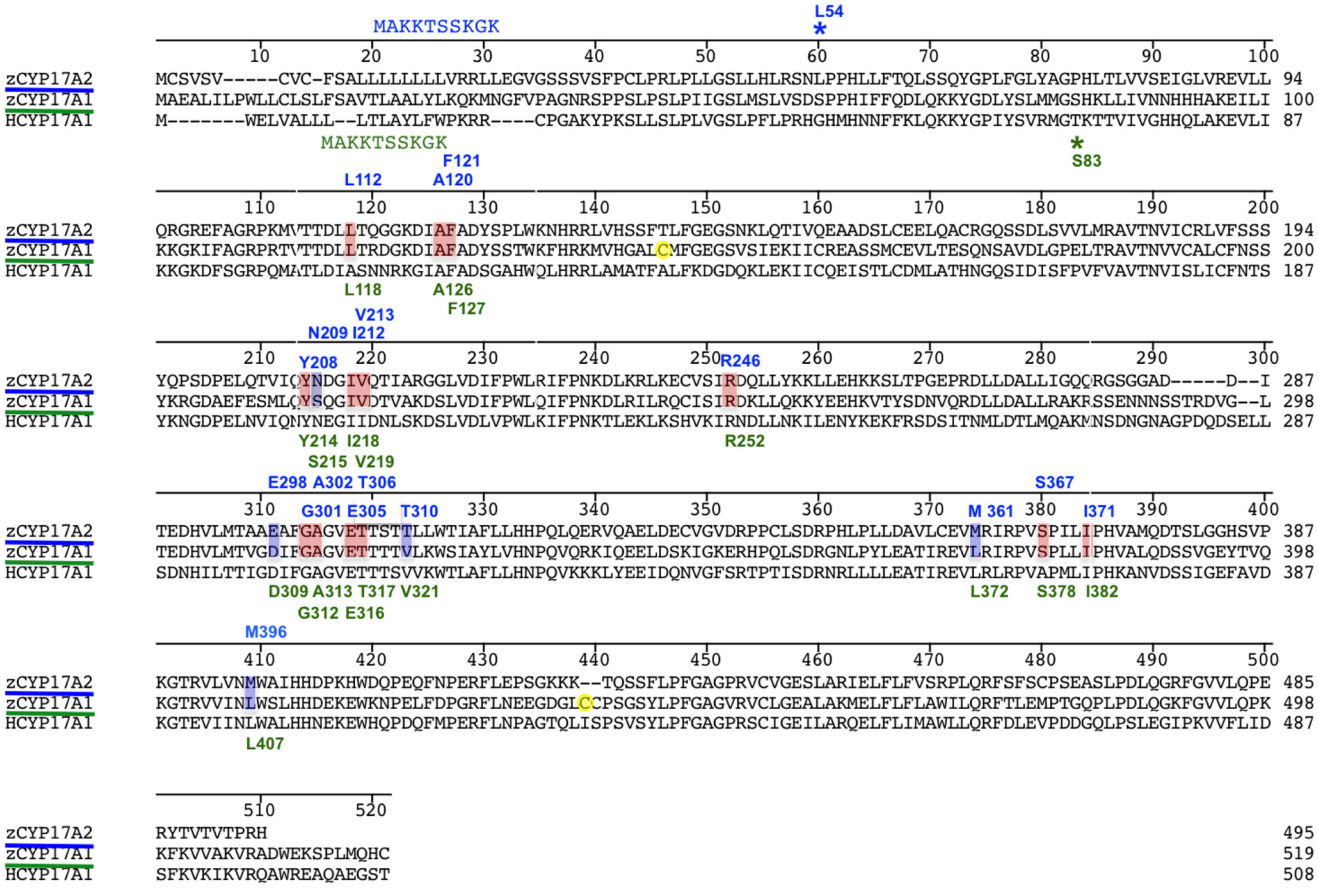

FIGURE 10. **Sequence alignments of the P450 17A1 and 17A2 proteins from zebrafish (*z*) and human (*h*) P450 17A1.** The alignment was generated with Clustal Omega (51). The pairwise identities between the proteins are as follows: z17A1 and z17A2, 51%; z17A1 and h17A1, 47%; z17A2 and h17A1, 42%. Active site amino acids in the crystal structures of the 17A1 and 17A2 P450s from zebrafish are labeled (in *green* and *blue*, respectively) and are highlighted in the two sequences in *blue* (different) or *red* (identical). *Asterisks* mark the N-terminal residues in the crystal structures (Leu-54 in the z17A2 complexes and Ser-83 in the z17A1 complex). The MAKKTSSKGK leader sequence replacing the N-terminal 26 amino acids in z17A1 (25 amino acids in z17A2) is shown below and *above* the aligned sequences, and Cys-146 and Cys-437 (which form disulfide bridges in the crystal structure of the z17A1-abiraterone complex) are highlighted with *yellow circles*.

the H-bond was established to Ser-215 (Fig. 11*B*), and in the P450 17A2 complex, the H-bond partner of the O3 hydrogen of abiraterone was Asn-209 (Fig. 12*B*).

Comparison between the Zebrafish P450 17A1 and 17A2 Active Sites—At both the levels of overall structure and active site conformation, the zebrafish 17A1 and 17A2 P450s displayed close similarities (Figs. 11–14), consistent with the 51% identity of their sequences (Fig. 10). The structural similarities extend to human P450 17A1 (Fig. 14, *A* and *B*), with sequence identities between the human P450 17A1 protein and zebrafish P450 17A1 and 17A2 of 47 and 42%, respectively (Fig. 10). Thus, there are no obvious differences in the active site conformations or volumes that discern the different enzymatic activities of the P450 17A1 (hydroxylation and lyase) and 17A2 proteins (hydroxylation only). Active site residues surrounding abiraterone or progesterone in the three crystal structures of P450 17A1 and 17A2 complexes are highlighted in Fig. 15. As is readily apparent, the majority of these amino acids are conserved between zebrafish P450 17A1 and 17A2, and the sequence identity among active site residues is ~75%. The five amino acid pairs that differ between P450 17A1 and A2 are highlighted in *blue* in Fig. 10 and include the following: Ser-215 (A1)/Asn-209 (A2), Asp-309/Glu-298, Val-321/Thr-310, Leu-372/Met-361, and Leu-407/Met-396. An overlay of the active sites in the 17A1 and A2 complexes with abiraterone and progesterone and the side chains of the residues that differ between the two P450s is depicted in Fig. 15. Four of the five residues that differ between P450 17A1 and 17A2 map to the vicinity of the heme, and interestingly, zebrafish and human P450 17A1 (which have both hydroxylation and lyase activity) exhibit matching amino acids at these positions (Fig. 10). None of the four altered side chains are in direct contact with progesterone in the crystal structure of the 17A2 complex. Rather, their locations are more suggestive of an association with the heme moiety. In particular, Met-361 (and the corresponding Leu-372 of P450 17A1) and Met-396 at the active site of P450 17A2 engage in hydrophobic interactions with the porphyrin ring (Fig. 15). The remaining divergent pair of amino acids, Ser-215 (P450 17A1) and Asn-209 (P450 17A2), is located at the opposite end of the active site, and both side chains form an H-bond to the hydroxyl group of abiraterone (Figs. 14 and 15). However, the amino acid in zebrafish P450 17A2 (Asn-209) matches that in human P450 17A1 (Asn-202) (Fig. 14, *B* and *D*). Obviously, in terms of a rationalization of the different catalytic activities of zebrafish and human P450 17A1 on the one hand and zebrafish P450 17A2 on the other hand, this active site position appears less interesting than the above four, with matching amino acids in the P450 17A1 proteins from human and zebrafish.

TABLE 4
Crystal data, data collection parameters, and structure refinement statistics

Complex	P450 17A1-abiraterone	P450 17A2-abiraterone	P450 17A2-progesterone
Data collection			
Wavelength (Å)]	1.73410	1.00395	0.97872
Space group	$P3_121$	$P2_1$	$P2_1$
Resolution (Å)	29.00-3.30	42.32-2.86	49.00-2.73
Outer shell (Å)	3.42-3.30[a]	2.94-2.86	2.81-2.73
Unit cell constants (Å)	136.63, 136.63, 135.44	57.01, 79.77, 95.24	55.94, 78.63, 95.41
Unique reflections	22,332 (2,192)	19,692 (1,417)	22,643 (1,655)
Completeness (%)	100 (100)	99.3 (99.5)	99.8 (99.9)
$I/\sigma(I)$	56.2 (11.9)	23.73 (4.29)	48.99 (2.73)
R-merge	0.111 (0.451)	0.099 (0.785)	0.074 (0.668)
Redundancy	21.7 (22.2)	7.4 (5.9)	4.7 (4.8)
Refinement			
Phasing method	Single anomalous dispersion (Fe)	Single anomalous dispersion (Fe/Hg)	Molecular replacement
R-work	0.171 (0.225)	0.222 (0.314)	0.206 (0.283)
R-free	0.233 (0.283)	0.304 (0.438)	0.288 (0.366)
No. of amino acids	828[b]	848[c]	845[d]
No. of protein atoms	6,481	6,399	6,595
No. of heme atoms	86	86	86
No. of ligand atoms	52	46	46
Average *B*-factor, protein atoms (Å^2)	73.4	88.7	60.7
Average *B*-factor, ligand/heme atoms (Å^2)	58.6/51.4	64.6/50.2	42.7/25.5
Wilson *B*-factor (Å^2)	75.9	79.5	53.3
r.m.s.d. bond lengths (Å)	0.013	0.015	0.011
r.m.s.d. bond angles (°)	1.8	1.7	1.7
Ramachandran plot: No. of favored/allowed residues/outliers	725/71/21	800/45/23	770/44/17
Protein Data Bank code	4R1Z	4R20	4R21

[a] Statistics for the highest resolution shell are shown in parentheses.
[b] For molecule A, residues 83–226/233–289/295–510; for molecule B, 83–230/241–289/295–508.
[c] For molecule A, residues 55–140/145–194/198–218/236–257/262–420/428–495; for molecule B, 53–141/148–218/235–418/427–496.
[d] For molecule A, residues 53–224/234–419/428–494; for molecule B, 53–220/233–420/427–493.

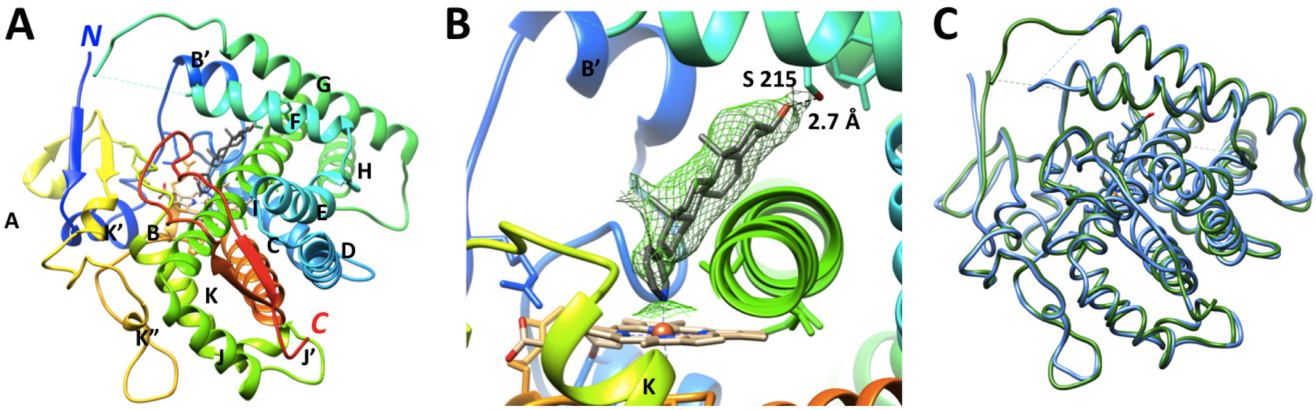

FIGURE 11. **Crystal structure of zebrafish P450 17A1 in complex with abiraterone.** *A*, overall view of the structure of the complex (molecule A), with the protein shown in *rainbow coloring*, from N terminus (*blue*) to C terminus (*red*). Carbon, nitrogen, and oxygen atoms of the heme moiety are colored in *beige, blue,* and *red*, respectively, and Fe^{3+} is shown as an *orange sphere*. Carbon and oxygen atoms of abiraterone are colored in *gray* and *red*, respectively. *B*, close-up view of the active site, with Fourier $2F_o - F_c$ omit electron density (1.2 σ level) around the inhibitor. A hydrogen bond between the hydroxyl group of abiraterone and Ser-215 is indicated with a *dashed line*. *C*, superimposition of the two independent complexes per crystallographic asymmetric unit (complex A is *cyan* and complex B is *green*). The r.m.s.d. between the two models is 0.47 Å.

Packing Features of the Zebrafish P450 17A1 and 17A2 Crystal Structures—In the crystal structures of the P450 17A1 and 17A2 complexes, the asymmetric unit consists of two independent P450 molecules with bound inhibitor or substrate (17A2). Both in the trigonal crystal system adopted by P450 17A1 and the monoclinic one adopted by P450 17A2 (Table 4), the two independent complexes are related via a noncrystallographic 2-fold rotation axis. In the P450 17A1·abiraterone structure complexes A and B dimerize with formation of two disulfide bridges, the first between Cys-146(A) and Cys-146(B) and the second between Cys-437(A) and Cys-437(B) (Fig. 16). Thus, disulfide bridges are oriented more or less perpendicularly to the noncrystallographic dyad. In the zebrafish P450 17A1 sequence, amino acid 438 is also a cysteine, but this residue is not involved in a disulfide bond. Neither human P450 17A1 nor zebrafish P450 17A2 features cysteine at the equivalent locations (Fig. 10).

DISCUSSION

The existence of P450 17A1 and 17A2 genes in fish provides an interesting approach to delineate the molecular basis of the 17α,20-lyase activity. We were able to confirm and extend the cell culture results of Zhou *et al.* (28) in greater detail, including extensive kinetic analysis and structural studies. Even though human P450 17A1 and the zebrafish P450s 17A1 and 17A2 are only ~50% identical (for any two comparisons of three proteins, Fig. 10), the active sites of the crystal structures are remarkably similar (Figs. 14 and 15).

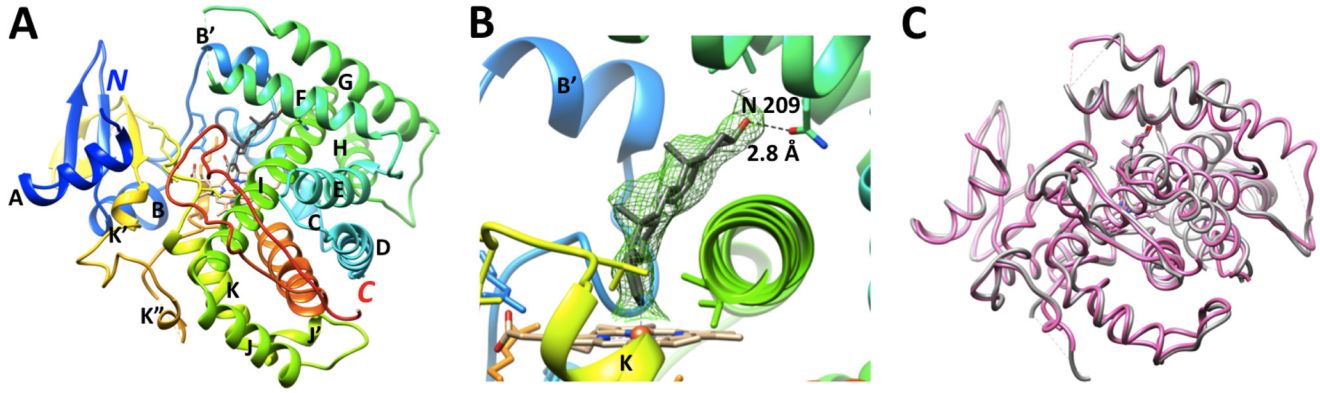

FIGURE 12. **Crystal structure of zebrafish P450 17A2 in complex with abiraterone.** *A*, overall view of the structure of the complex (molecule A); the color code matches that in Fig. 11. *B*, close-up view of the active site, with Fourier $2F_o - F_c$ omit electron density (1.2 σ level) around the inhibitor. A hydrogen bond between the hydroxyl group of abiraterone and Asn-209 is indicated by a *dashed line*. *C*, superimposition of the two independent complexes per crystallographic asymmetric unit (complex A is *pink* and complex B is *gray*). The r.m.s.d. between the two models is 0.58 Å.

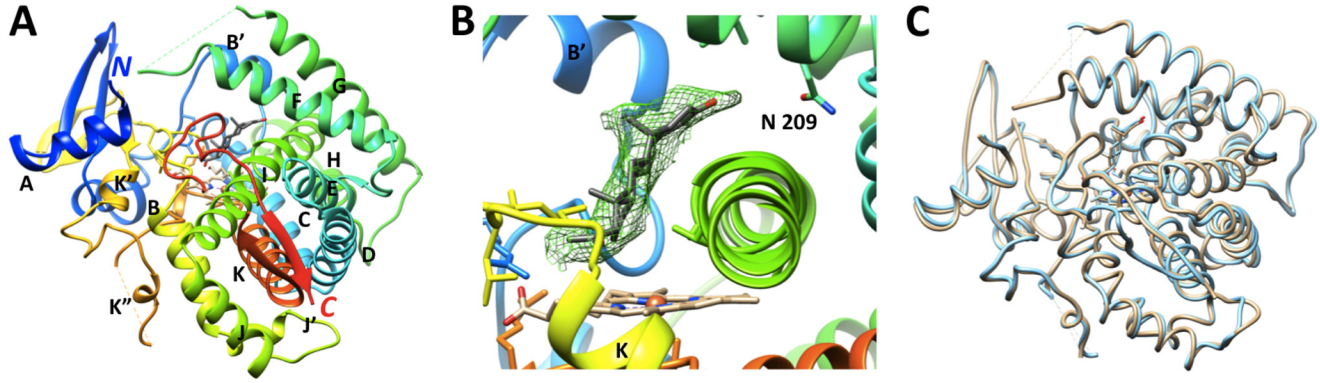

FIGURE 13. **Crystal structure of zebrafish P450 17A2 in complex with progesterone.** *A*, overall view of the structure of the complex (molecule A); the color code matches that in Fig. 11. Carbon and oxygen atoms of progesterone are colored in *gray* and *red*, respectively. *B*, close-up view of the active site, with Fourier $2F_o - F_c$ omit electron density (1.2 σ level) around the substrate. *C*, superimposition of the two independent complexes per crystallographic asymmetric unit (complex A is *cyan* and complex B is *beige*). The r.m.s.d. between the two models is 0.56 Å.

We confirmed the report of Zhou *et al.* (28) regarding the catalytic selectivity of tilapia P450 17A1 and 17A2 (termed P450c17-I and -II in that paper) in zebrafish. P450 17A1 had also been cloned from zebrafish (55) and sole (56). Because both enzymes are expressed in several teleost fish (28), we presume that the pattern is general in these fish. P450 17A1 is expressed in the ovary and is proposed to be involved in synthesis of 17β-estradiol, and P450 17A2 is localized in what is termed the head kidney and proposed to be involved in the production of C21 steroids, *e.g.* cortisol (28). (The head kidney (most cranial portion of kidney) contains predominantly hematopoietic and lymphoid tissue; the posterior kidney contains the excretory tissue with some hematopoietic and lymphoid tissue.) Temporal switching from P450 17A1 to 17A2 expression has also been observed (28) and has been proposed to be related to a change from production of 17β-estradiol to the C21 steroid 17α,20β-dihydroxy-4-pregnen-3-one (a maturation-inducing hormone) in fish ovaries (28). P450 17A2 is thus suggested to be involved in the production of hormones that induce oocyte maturation in fish (28).

At the outset of the project, we hypothesized that the difference between fish P450 17A1 and 17A2, *i.e.* 17α,20-lyase activity, might be attributable to one or a few structural changes that facilitate binding of 17α-OH steroids in P450 17A1 (as a substrate) but not in P450 17A2. However, this is not the case, in that (i) P450 17A2 bound the 17α-OH steroids nearly as well (progesterone) or better (pregnenolone) than the parent steroids (Table 2), and (ii) overlays of the crystal structures (Fig. 15) reveal only small differences between the proteins, and these do not appear to directly affect ligand binding.

With the available information, we can consider two hypotheses for the presence of 17α,20-lyase activity in fish P450 17A1 but not P450 17A2. (i) Five residues are altered in fish P450 17A2 compared with fish 17A1 (four compared with human P450 17A1), and four of these are near the periphery of the heme prosthetic group (Fig. 15; Glu-298, Thr-310, Met-361, and Met-396 (17A2 numbering)). There is experimental support for the involvement of a nucleophilic $Fe^{(II)}O_2^-$ entity (ferric peroxide) in the 17α,20-lyase mechanism (9–11, 57, 58). It is possible that the (four) residues that contact the heme periphery are necessary for the heme to utilize the ferric peroxide mechanism, *e.g.* by stabilizing the iron in the ferric peroxide state (in the presence of a 17α-OH steroid). The FeO^{3+} (compound I) entity could be used by both P450 17A1 and 17A2 in the 17α-hydroxylation reactions. Perhaps consistent with this view is the more efficient pregnenolone 17α-hydroxylation reaction with P450 17A2 (Table 1), which might be the result of an enhanced conversion of the ferric peroxide ($Fe^{(II)}O_2^-$) to compound I in the catalytic cycle. However, we were unable to

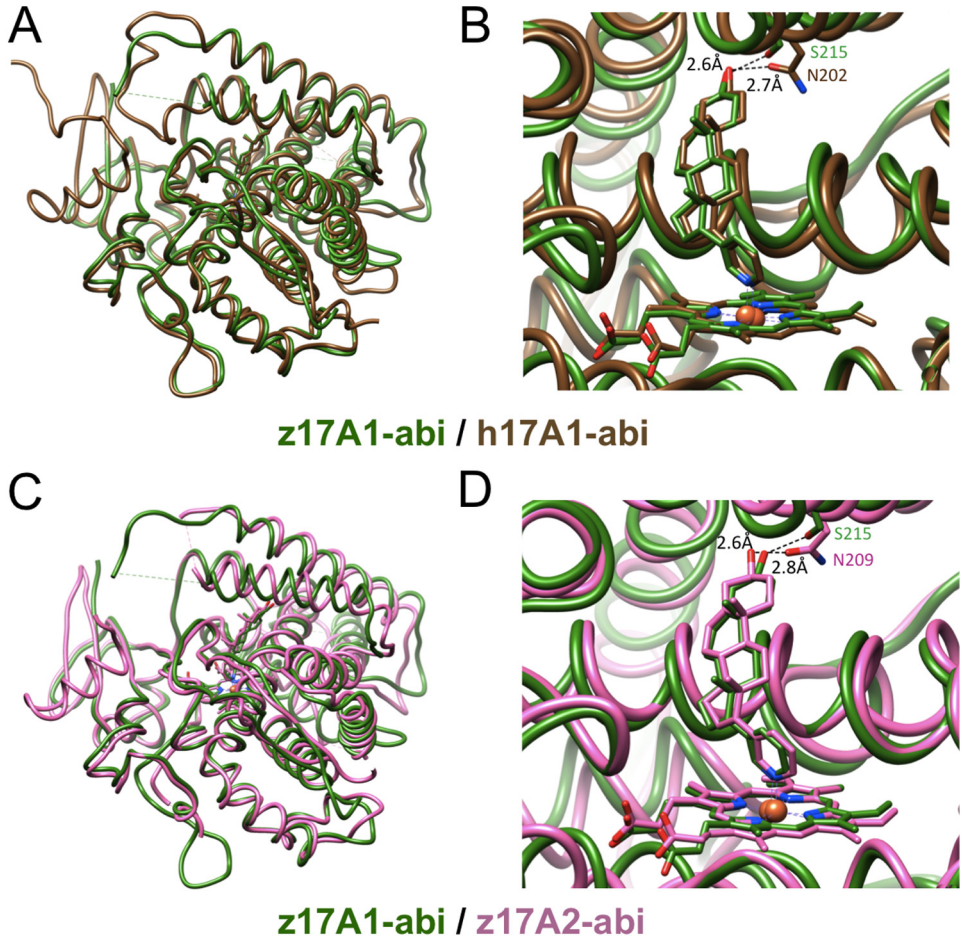

FIGURE 14. **Comparisons between the crystal structures of the zebrafish P450 17A1 and 17A2 and human P450 17A1 abiraterone complexes.** *A*, overall view of the superimposed z17A1 (*green*) and h17A1 (*brown*) complexes; the r.m.s.d. between the two models amounts to 1.35 Å. *B*, close-up view of the active sites, revealing similar orientations of the inhibitor in the two structures. *C*, overall view of the superimposed zebrafish (*z*) P450 17A1 (*green*) and z17A2 (*pink*) complexes; the r.m.s.d. between the two models amounts to 1.49 Å. *D*, close-up view of the active sites, revealing similar orientations of the inhibitor in the two structures. *Dashed lines* indicate hydrogen bonds.

detect any spectroscopic differences in the heme (Soret band) between (ferric) P450 17A1 and 17A2 (UV-visible or circular dichroism, results not presented). (ii) An alternative possibility comes from the recent report of Estrada *et al.* (59) that NMR spectra of human P450 17A1 show multiple two-dimensional signals, interpreted as evidence of multiple conformations of the enzyme. The equilibrium of these conformations is believed to be affected by the presence of b_5 (59). In considering fish P450 17A1 and 17A2, it is possible that P450 17A1 adopts additional conformations (compared with P450 17A2), allowing it to catalyze the 17α,20-lyase reaction in addition to 17α-hydroxylation.

It is known that human P450 17A1 displays an efficient lyase activity with 17α-OH pregnenolone, whereas 17α-OH progesterone is a poor substrate for the lyase (60). Recently reported crystal structures of human 17A1·substrate complexes revealed that both pregnenolone and progesterone adopt an active site position that allows formation of a hydrogen bond between their respective C3 alcohol and keto substituents and the side chain of Asn-202 (8). This is similar to the H-bond between Asn-202 and the hydroxyl group of abiraterone in the complex with human P450 17A1 (5) and the abiraterone complexes with zebrafish P450 17A1 (Ser-215; Fig. 11) and 17A2 (Asn-209; Fig. 12). However, in our complex between progesterone and the zebrafish P450 17A2, the substrate is too far removed from Asn-209 to establish an H-bond (Fig. 13). Interestingly, in the crystal structures of human P450 17A1 with 17α-OH pregnenolone and 17α-OH progesterone, the latter substrate still forms the H-bond to Asn-202, whereas 17α-OH pregnenolone was found in two orientations (8). In one orientation, the H-bond between the hydroxyl group at C3 and Asn-202 is maintained, but in the other orientation the contact is severed, and the substrate for the lyase moved closer to the iron and the (putative) catalytic peroxy intermediate. This closer proximity may account for the facilitated human P450 17A1 lyase reaction with 17α-OH pregnenolone relative to 17α-OH progesterone. In the absence of structures of zebrafish P450 17A1 and 17A2 in complex with 17α-OH progesterone and 17α-OH pregnenolone, it is not possible to gauge the importance of the presence or absence of this H-bond for the ability of zebrafish P450 17A1 to catalyze the lyase reaction and the inability of P450 17A2 to do so. It is noteworthy, however, that the amino acids at position 202 (Asn) in human P450 17A1 (lyase activity) and at position 209 (Asn) in zebrafish P450 17A2 (no lyase activity) match (Fig. 10). Conversely, zebrafish P450 17A1, which possesses lyase activity with both 17α-OH progesterone and 17α-OH

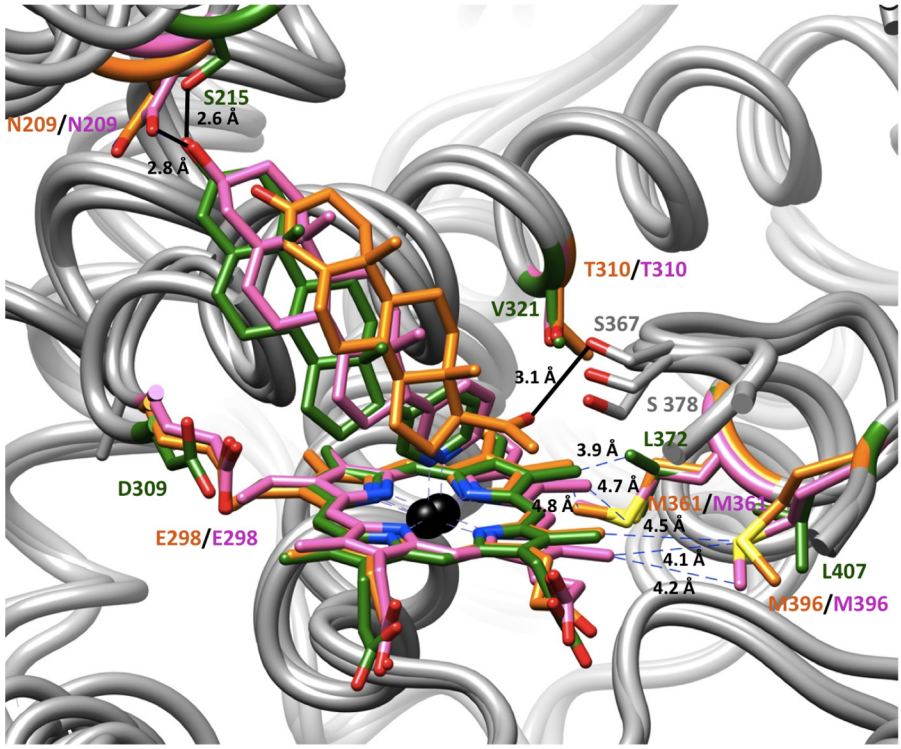

FIGURE 15. **Deviating orientations of abiraterone and progesterone and amino acid compositions at the active sites of zebrafish P450 17A1 and 17A2.** Superimposition of the zebrafish (*z*) P450 17A1 (*green*) and 17A2 (*pink*) abiraterone complexes and the P450 17A2 progesterone complex (*orange*). The heme moiety and side chains of active site residues that differ between the z17A1 and z17A2 proteins are depicted with the color of carbon atoms matching that of the inhibitor/substrate molecule and are labeled. *Solid black* and *dashed blue lines* indicate hydrogen bonds and selected hydrophobic contacts, respectively.

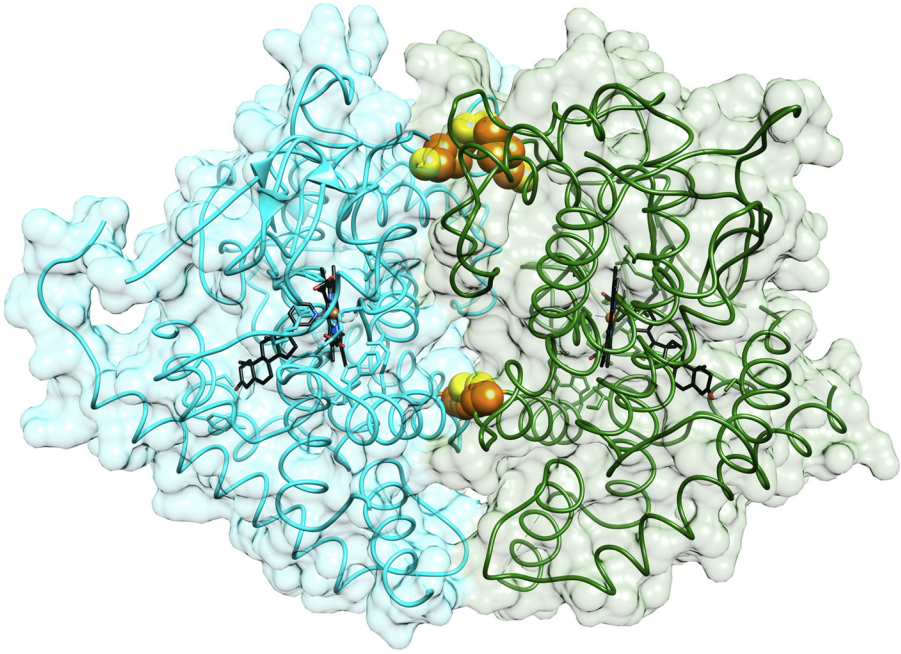

FIGURE 16. **Dimerization of zebrafish P450 17A1·abiraterone complexes with formation of two disulfide bonds.** The view is approximately along the normal to the noncrystallographic 2-fold rotation axis that runs from top to bottom and relates complexes A (*cyan*) and B (*green*) that constitute the crystallographic asymmetric unit. The two disulfide bridges are formed between Cys-146(A) and Cys-146(B) (*bottom*) and Cys-437(A) and Cys-437(B) (*top*). Another cysteine pair (Cys-438) at the dimerization interface does not form a disulfide bond. Cysteines are shown in space-filling mode with carbon and sulfur atoms colored in *orange* and *yellow*, respectively, and heme and abiraterone are shown in *ball-and-stick* mode with carbon atoms colored in *black*.

pregnenolone, features serine in the equivalent location (Ser-215).

17α-OH progesterone and 17α-OH pregnenolone are both products and substrates for P450 17A1 enzymes. There has been consideration of the processivity of the overall reaction (19–23, 26) as in the case of numerous other P450 reactions (4, 61–66). In this case, we were able to address the processivity of the zebrafish P450 17A1 reactions using several kinetic

approaches. The pregnenolone reaction (forming DHEA) was definitely more processive than the progesterone reaction (forming androstenedione). A lag phase was seen in the two-step progesterone reaction but not for pregnenolone oxidation (Figs. 3, *A* and *B*, and 8, *A* and *B*). The weaker inhibition of label incorporation by 17α-OH steroid in the case of the conversion of pregnenolone to DHEA (Fig. 4, *C* and *D*) is also consistent with this conclusion. The measured K_d (Table 2) and k_{off} (Fig. 5, *E* and *G*) values also indicate that 17α-OH pregnenolone is bound to zebrafish P450 17A1 more tightly than is 17α-OH progesterone. The selectivity of orteronel for inhibiting the more distributive progesterone oxidation (Table 3) is also consistent.

We used experimental results (K_d, k_{off}, and k_{cat}) to seed a model, generated to fit multiple kinetic data sets in a pulse-chase experiment (Fig. 8). The result (Fig. 9), with its estimated rate constants, yields values that may reflect the balance in a qualitatively similar way (as in Fig. 7) but be more appropriate, in that k_{cat} values can be misleading due to the contribution of multiple steps (67, 68). The ratio of the estimated rate of conversion of 17α-OH progesterone (to androstenedione) to its k_{off} rate was ~0.1, whereas the value for conversion of 17α-OH pregnenolone to its k_{off} rate was ~2. Thus, one interpretation of these values is that zebrafish P450 17A1 is 20-fold more processive in the case of 17α-OH pregnenolone than 17α-OH progesterone (Fig. 9). For bovine P450 17A1, Yamazaki *et al.* (19) used a different approach to calculate corresponding ratios of 0.6 and 5 (*cf.* 0.1 and 2 in our case, see above), yielding a processivity ratio of ~8 (5/0.6). Thus, both the zebrafish and bovine P450 17A1 are more processive in the pregnenolone than the progesterone reaction, as observed qualitatively (Figs. 3 and 5 and Table 3) and with calculations (Figs. 6, 7, and 9). The main reason appears to be the difference in the dissociation rates of the 17α-OH steroids (Figs. 5, 6, and 8).

Kinetic studies with P450 17A1 from other species have been reported, using other approaches. Yamazaki *et al.* (24, 25) concluded that the reactions were processive in cultured bovine adrenocortical cells and rat ovarian microsomes. Tagashira *et al.* (26) concluded that the oxidation of progesterone to androstenedione by guinea pig P450 17A1 was processive and that the rate-limiting step was product dissociation. Yamazaki *et al.* (19), using similar approaches in the same laboratory, concluded that ~20% of 17α-OH pregnenolone did not dissociate from bovine P450 17A1 in the oxidation of pregnenolone to DHEA. In both cases, reactions were considered to be limited by product k_{off} rates. If this is true, one would expect to observe burst kinetics for product formation (69), but such experiments were not performed. In our work with zebrafish P450 17A1, none of the reactions appear to be limited by k_{off} rates (Figs. 7 and 8). The rates of dissociation of products were faster than k_{cat} values for formation.

One of the possibilities for the stimulatory effect of b_5 on 17α,20-lyase reactions could be that it slows the release of 17α-OH steroids from P450 17A1, thus favoring further reactions (Fig. 1). However, the presence of b_5 did not significantly affect the rate of 17α-OH pregnenolone release from zebrafish P450 17A1 (Fig. 6*H*). Whether this is true in P450 17A1 from other animals is unknown, and the zebrafish stimulation by b_5 (Fig. 3) is less than with human P450 17A1 (12, 13).

One of the features of the P450 17A2 reaction with pregnenolone is that it did not proceed to completion (Fig. 3*D*), stopping after about 60% of the substrate had been converted to the 17α-OH product. We searched for possible further oxidation products that might have been overlooked, but we found none. We propose that the higher affinity of the P450 17A2 product for the enzyme, relative to substrate (4-fold, Table 2), had the effect of slowing the reaction.

The experimental drug orteronel has been shown to preferentially inhibit the 17α-OH pregnenolone lyase activity of human P450 17A1 (7). This was the case with progesterone oxidations with fish P450 17A1 but not pregnenolone (Table 3). Interestingly, orteronel was a strong inhibitor of fish P450 17A2-catalyzed 17α-hydroxylation of progesterone but not pregnenolone (Table 3). The reasons for the higher IC_{50} values for progesterone 17α-hydroxylation by zebrafish P450 17A1 and pregnenolone 17α-hydroxylation by P450 17A2 are not clear. However, the differential IC_{50} values for zebrafish P450 17A1 in inhibiting progesterone 17α-hydroxylation and 17α,20-lyase activity can be viewed as being consistent with the more distributive nature of progesterone oxidation (Fig. 9). Marked species variation of the inhibitory action of orteronel have been reported elsewhere (70). We conclude the following: (i) in the fish systems, the action of orteronel on P450 17A1 would be to block androstenedione production, and (ii) that, at least with progesterone, the oxidation is distributive, supporting the conclusion with kinetic studies (Figs. 5–9).

Work with clinically observed cases of endocrine insufficiency has shown that a single amino acid change can cause the selective loss of the lyase activity of human P450 17A1 (2, 71). Thus, it can be stated that the fish P450 17A1 residue corresponding to human P450 17A1 Arg-358 is essential for the lyase activity, although the reason is not yet clear. Preliminary site-directed mutagenesis work with the zebrafish P450 17A enzymes showed that the change R369C with P450 17A1 (corresponding to human P450 17A1 R358C) abolished its lyase activity, consistent with the preferential loss of 17α,20-lyase activity in human P450 17A1 Arg-347 and Arg-358 variants, but making the change C358R did not produce lyase activity in P450 17A2 (results not shown). We propose that this amino acid residue of P450 17A1 is necessary for the lyase activity (although others may also cause this) and that multiple substitutions of P450 17A2 are probably needed to confer lyase activity to this protein. Human P450 17A1 Arg-358 has been implicated in b_5 binding through NMR, chemical cross-linking, and other techniques (59, 72, 73). However, zebrafish P450 17A1 shows only ~2-fold stimulation by b_5 (Fig. 3*B*), and it is not clear whether another mechanism is involved in the loss of lyase activity conferred by the mutation at Arg-369 (equivalent of human P450 17A1 Arg-358).

The sequence identity between zebrafish P450 17A1 and 17A2 is only ~51%, and they are only classified in the same P450 gene subfamily by exception to the normal cutoff value of 55%. Despite the lack of the 17α,20-lyase activity in P450 17A2, the conservations of both active site structure (Figs. 10, 15) and catalytic selectivity (17α-hydroxylation, Table 1) are somewhat

remarkable for P450s with such limited similarity (3, 4). Although some examples of P450s from different gene subfamilies and families catalyzing the same reaction with xenobiotic substrates (*e.g.* drugs) are known, there are few good examples of similar activity with endogenous compounds (including vitamins), and some of these may be the result of chemical reactivity more than specific binding. 25-Hydroxylation of vitamin D_3 is catalyzed by a number of P450s (74). Another example is retinoic acid 4-hydroxylation (75), which may be due in part to the chemical proclivity of oxidation at the allylic position. A number of P450s also catalyze ω-hydroxylation of fatty acids, but this is probably due to steric restriction (76). However, in these cases it is highly unlikely that the structures of the active sites are so similar as those of P450s 17A1 and 17A2 (Figs. 10 and 15).

In summary, we have characterized several aspects of zebrafish P450 17A1 and 17A2. These proteins are only 51% identical, but both efficiently catalyze steroid 17α-hydroxylation (Table 1) and have very similar active site structures (Fig. 15). The active site changes that allow for only P450 17A1 to catalyze the 17α,20-lyase reaction are small, and either the reason for the differences is the subtle changes or else switches in residues removed from the heme region (Fig. 15). Several lines of kinetic evidence indicate that the P450 17A1 two-step oxidations of both progesterone and pregnenolone are partially distributive, but the processivity is greater with pregnenolone due to a 10-fold lower k_{off} rate for 17α-OH pregnenolone (than 17α-OH progesterone) (Table 2 and Figs. 6, 7, and 9). The relevance of these findings to mammalian P450 17A1 enzymes, which vary in many of their catalytic properties for the Δ^4 and Δ^5 steroids (19, 77), is under investigation.

Acknowledgments—We thank Millennium Pharmaceuticals for orteronel, J. A. Oates for use of the radio-TLC imaging scanner, and K. Trisler for assistance in preparation of the manuscript. Vanderbilt University is a member institution of the Life Sciences Collaborative Access Team (LS-CAT) at Sector 21 of the Advanced Photon Source (APS), Argonne, IL. Use of the APS at Argonne National Laboratory was supported by the United States Department of Energy, Office of Science, Office of Basic Energy Sciences, under Contract DE-AC02-06CH11357.

REFERENCES

1. Ortiz de Montellano, P. R. (ed) (2005) *Cytochrome P450: Structure, Mechanism, and Biochemistry*, 3rd Ed., Kluwer Academic/Plenum Publishers, New York
2. Miller, W. L., and Auchus, R. J. (2011) The molecular biology, biochemistry, and physiology of human steroidogenesis and its disorders. *Endocr. Rev.* **32,** 81–151
3. Guengerich, F. P. (2005) in *Cytochrome P450: Structure, Mechanism, and Biochemistry* (Ortiz de Montellano, P. R., ed) 3rd Ed., pp. 377–530, Kluwer Academic/Plenum Press, New York
4. Guengerich, F. P. (2015) in *Cytochrome P450: Structure, Mechanism, and Biochemistry* (Ortiz de Montellano, P. R., ed.), 4th Ed., Springer-Verlag, in press
5. DeVore, N. M., and Scott, E. E. (2012) Structures of cytochrome P450 17A1 with prostate cancer drugs abiraterone and TOK-001. *Nature* **482,** 116–119
6. Kaku, T., Hitaka, T., Ojida, A., Matsunaga, N., Adachi, M., Tanaka, T., Hara, T., Yamaoka, M., Kusaka, M., Okuda, T., Asahi, S., Furuya, S., and Tasaka, A. (2011) Discovery of orteronel (TAK-700), a naphthylmethylimidazole derivative, as a highly selective 17,20-lyase inhibitor with potential utility in the treatment of prostate cancer. *Bioorg. Med. Chem.* **19,** 6383–6399
7. Yamaoka, M., Hara, T., Hitaka, T., Kaku, T., Takeuchi, T., Takahashi, J., Asahi, S., Miki, H., Tasaka, A., and Kusaka, M. (2012) Orteronel (TAK-700), a novel non-steroidal 17,20-lyase inhibitor: effects on steroid synthesis in human and monkey adrenal cells and serum steroid levels in cynomolgus monkeys. *J. Steroid Biochem. Mol. Biol.* **129,** 115–128
8. Petrunak, E. M., DeVore, N. M., Porubsky, P. R., and Scott, E. E. (2014) Structures of human steroidogenic cytochrome P450 17A1 with substrates. *J. Biol. Chem.* **289,** 32952–32964
9. Akhtar, M., Corina, D., Miller, S., Shyadehi, A. Z., and Wright, J. N. (1994) Mechanism of the acyl-carbon cleavage and related reactions catalyzed by multifunctional P-450s: studies on cytochrome P45017α. *Biochemistry* **33,** 4410–4418
10. Gregory, M. C., Denisov, I. G., Grinkova, Y. V., Khatri, Y., and Sligar, S. G. (2013) Kinetic solvent isotope effect in human P450 CYP17A1-mediated androgen formation: evidence for a reactive peroxoanion intermediate. *J. Am. Chem. Soc.* **135,** 16245–16247
11. Gregory, M., Mak, P. J., Sligar, S. G., and Kincaid, J. R. (2013) Differential hydrogen bonding in human CYP17 dictates hydroxylation *versus* lyase chemistry. *Angew. Chem. Int. Ed. Engl.* **52,** 5342–5345
12. Katagiri, M., Suhara, K., Shiroo, M., and Fujimura, Y. (1982) Role of cytochrome b_5 in the cytochrome P-450-mediated C21-steroid 17,20-lyase reaction. *Biochem. Biophys. Res. Commun.* **108,** 379–384
13. Katagiri, M., Kagawa, N., and Waterman, M. R. (1995) The role of cytochrome b_5 in the biosynthesis of androgens by human P450c17. *Arch. Biochem. Biophys.* **317,** 343–347
14. Zhang, L. H., Rodriguez, H., Ohno, S., and Miller, W. L. (1995) Serine phosphorylation of human P450c17 increases 17,20-lyase activity: implications for adrenarche and the polycystic ovary syndrome. *Proc. Natl. Acad. Sci. U.S.A.* **92,** 10619–10623
15. Tee, M. K., Dong, Q., and Miller, W. L. (2008) Pathways leading to phosphorylation of P450c17 and to the posttranslational regulation of androgen biosynthesis. *Endocrinology* **149,** 2667–2677
16. Tee, M. K., and Miller, W. L. (2013) Phosphorylation of human cytochrome P450c17 by p38α selectively increases 17,20-lyase activity and androgen biosynthesis. *J. Biol. Chem.* **288,** 23903–23913
17. Auchus, R. J., Lee, T. C., and Miller, W. L. (1998) Cytochrome b_5 augments the 17,20-lyase activity of human P450c17 without direct electron transfer. *J. Biol. Chem.* **273,** 3158–3165
18. Estrada, D. F., Laurence, J. S., and Scott, E. E. (2013) Substrate-modulated cytochrome P450 17A1 and cytochrome b_5 interactions revealed by NMR. *J. Biol. Chem.* **288,** 17008–17018
19. Yamazaki, T., Ohno, T., Sakaki, T., Akiyoshi-Shibata, M., Yabusaki, Y., Imai, T., and Kominami, S. (1998) Kinetic anaylsis of successive reactions catalyzed by bovine cytochrome $P450_{17\alpha,lyase}$. *Biochemistry* **37,** 2800–2806
20. Soucy, P., and Luu-The, V. (2000) Conversion of pregnenolone to DHEA by human 17α-hydroxylase/17,20-lyase (P450c17). Evidence that DHEA is produced from the released intermediate, 17α-hydroxypregnenolone. *Eur. J. Biochem.* **267,** 3243–3247
21. Higuchi, A., Kominami, S., and Takemori, S. (1991) Kinetic control of steroidogenesis by steroid concentration in guinea pig adrenal microsomes. *Biochim. Biophys. Acta* **1084,** 240–246
22. Kühn-Velten, W. N., Bunse, T., and Förster, M. E. (1991) Enzyme kinetic and inhibition analyses of cytochrome P450XVII, a protein with a bifunctional catalytic site: quantification of effective substrate concentrations at the active site and their significance for intrinsic control of the hydroxylase/lyase reaction sequence. *J. Biol. Chem.* **266,** 6291–6301
23. Swinney, D. C., and Mak, A. Y. (1994) Androgen formation by cytochrome P450 CYP17. Solvent isotope effect and pL studies suggest a role for protons in the regulation of oxene *versus* peroxide chemistry. *Biochemistry* **33,** 2185–2190
24. Yamazaki, T., Nawa, K., Kominami, S., and Takemori, S. (1992) Cytochrome $P\text{-}450_{17\alpha,\,lyase}$-mediating pathway of androgen synthesis in bovine adrenocortical cultured cells. *Biochim. Biophys. Acta* **1134,** 143–148
25. Yamazaki, T., Marumoto, T., Kominami, S., Ishimura, K., Yamamoto, A.,

and Takemori, S. (1992) Kinetic studies on androstenedione production in ovarian microsomes from immature rats. *Biochim. Biophys. Acta* **1125,** 335–340
26. Tagashira, H., Kominami, S., and Takemori, S. (1995) Kinetic studies of cytochrome $P450_{17\alpha,lyase}$ dependent androstenedione formation from progesterone. *Biochemistry* **34,** 10939–10945
27. Brock, B. J., and Waterman, M. R. (1999) Biochemical differences between rat and human cytochrome P450c17 support the different steroidogenic needs of these two species. *Biochemistry* **38,** 1598–1606
28. Zhou, L. Y., Wang, D. S., Kobayashi, T., Yano, A., Paul-Prasanth, B., Suzuki, A., Sakai, F., and Nagahama, Y. (2007) A novel type of P450c17 lacking the lyase activity is responsible for C21-steroid biosynthesis in the fish ovary and head kidney. *Endocrinology* **148,** 4282–4291
29. Hanna, I. H., Teiber, J. F., Kokones, K. L., and Hollenberg, P. F. (1998) Role of the alanine at position 363 of cytochrome P450 2B2 in influencing the NADPH- and hydroperoxide-supported activities. *Arch. Biochem. Biophys.* **350,** 324–332
30. Guengerich, F. P. (2005) Reduction of cytochrome b_5 by NADPH-cytochrome P450 reductase. *Arch. Biochem. Biophys.* **440,** 204–211
31. Shimada, T., Misono, K. S., and Guengerich, F. P. (1986) Human liver microsomal cytochrome P-450 mephenytoin 4-hydroxylase, a prototype of genetic polymorphism in oxidative drug metabolism. Purification and characterization of two similar forms involved in the reaction. *J. Biol. Chem.* **261,** 909–921
32. Richardson, T. H., Jung, F., Griffin, K. J., Wester, M., Raucy, J. L., Kemper, B., Bornheim, L. M., Hassett, C., Omiecinski, C. J., and Johnson, E. F. (1995) A universal approach to the expression of human and rabbit cytochrome P450s of the 2C subfamily in *Escherichia coli*. *Arch. Biochem. Biophys.* **323,** 87–96
33. Nishihara, K., Kanemori, M., Kitagawa, M., Yanagi, H., and Yura, T. (1998) Chaperone coexpression plasmids: differential and synergistic roles of DnaK-DnaJ-GrpE and GroEL-GroES in assisting folding of an allergen of Japanese cedar pollen, Cryj2, in *Escherichia coli*. *Appl. Environ. Microbiol.* **64,** 1694–1699
34. Sandhu, P., Baba, T., and Guengerich, F. P. (1993) Expression of modified cytochrome P450 2C10 (2C9) in *Escherichia coli*, purification, and reconstitution of catalytic activity. *Arch. Biochem. Biophys.* **306,** 443–450
35. Omura, T., and Sato, R. (1964) The carbon monoxide-binding pigment of liver microsomes. I. Evidence for its hemoprotein nature. *J. Biol. Chem.* **239,** 2370–2378
36. Zhao, B., Lei, L., Kagawa, N., Sundaramoorthy, M., Banerjee, S., Nagy, L. D., Guengerich, F. P., and Waterman, M. R. (2012) Three-dimensional structure of steroid 21-hydroxylase (cytochrome P450 21A2) with two substrates reveals locations of disease-associated variants. *J. Biol. Chem.* **287,** 10613–10622
37. Strittmatter, P., Fleming, P., Connors, M., and Corcoran, D. (1978) Purification of cytochrome b_5. *Methods Enzymol.* **52,** 97–101
38. Olsen, J. V., Ong, S. E., and Mann, M. (2004) Trypsin cleaves exclusively C-terminal to arginine and lysine residues. *Mol. Cell. Proteomics* **3,** 608–614
39. Otwinowski, Z., and Minor, W. (1997) Processing of X-ray diffraction data collected in oscillation mode. *Methods Enzymol.* **276,** 307–326
40. Winter, G. (2010) xia2: an expert system for macromolecular crystallography data reduction. *J. Appl. Crystallogr.* **43,** 186–190
41. Evans, P. (2006) Scaling and assessment of data quality. *Acta Crystallogr. D Biol. Crystallogr.* **62,** 72–82
42. Adams, P. D., Afonine, P. V., Bunkóczi, G., Chen, V. B., Davis, I. W., Echols, N., Headd, J. J., Hung, L. W., Kapral, G. J., Grosse-Kunstleve, R. W., McCoy, A. J., Moriarty, N. W., Oeffner, R., Read, R. J., Richardson, D. C., Richardson, J. S., Terwilliger, T. C., and Zwart, P. H. (2010) PHENIX: a comprehensive Python-based system for macromolecular structure solution. *Acta Crystallogr. D Biol. Crystallogr.* **66,** 213–221
43. Emsley, P., and Cowtan, K. (2004) Coot: Model-building tools for molecular graphics. *Acta Crystallogr. D Biol. Crystallogr.* **60,** 2126–2132
44. Murshudov, G. N., Skubák, P., Lebedev, A. A., Pannu, N. S., Steiner, R. A., Nicholls, R. A., Winn, M. D., Long, F., and Vagin, A. A. (2011) REFMAC5 for the refinement of macromolecular crystal structures. *Acta Crystallogr. D Biol. Crystallogr.* **67,** 355–367
45. Collaborative Computational Project No. 4 (1994) The CCP4 suite: programs for protein crystallography. *Acta Crystallogr. D Biol. Crystallogr.* **50,** 760–763
46. McCoy, A. J., Grosse-Kunstleve, R. W., Adams, P. D., Winn, M. D., Storoni, L. C., and Read, R. J. (2007) Phaser crystallographic software. *J. Appl. Crystallogr.* **40,** 658–674
47. Guengerich, F. P. (2014) in *Hayes' Principles and Methods of Toxicology* (Hayes, A. W., and Kruger, C. L., eds) 6th Ed., pp. 1905–1964, CRC Press-Taylor & Francis, Boca Raton, FL
48. Johnson, K. A., Simpson, Z. B., and Blom, T. (2009) Global Kinetic Explorer: a new computer program for dynamic simulation and fitting of kinetic data. *Anal. Biochem.* **387,** 20–29
49. Hara, T., Kouno, J., Kaku, T., Takeuchi, T., Kusaka, M., Tasaka, A., and Yamaoka, M. (2013) Effect of a novel 17,20-lyase inhibitor, orteronel (TAK-700), on androgen synthesis in male rats. *J. Steroid Biochem. Mol. Biol.* **134,** 80–91
50. Fersht, A. (1999) *Structure and Mechanism in Protein Science*, pp. 158–168, W. H. Freeman & Co., New York
51. Sievers, F., Wilm, A., Dineen, D., Gibson, T. J., Karplus, K., Li, W., Lopez, R., McWilliam, H., Remmert, M., Söding, J., Thompson, J. D., and Higgins, D. G. (2011) Fast, scalable generation of high-quality protein multiple sequence alignments using Clustal Omega. *Mol. Syst. Biol.* **7,** 539
52. Dong, A., Xu, X., Edwards, A. M., Midwest Center for Structural Genomics, Structural Genomics Consortium, Chang, C., Chruszcz, M., Cuff, M., Cymborowski, M., Di Leo, R., Egorova, O., Evdokimova, E., Filippova, E., Gu, J., Guthrie, J., Ignatchenko, A., Joachimiak, A., Klostermann, N., Kim, Y., Korniyenko, Y., Minor, W., Que, Q., Savchenko, A., Skarina, T., Tan, K., Yakunin, A., Yee, A., Yim, V., Zhang, R., Zheng, H., Akutsu, M., Arrowsmith, C., Avvakumov, G. V., Bochkarev, A., Dahlgren, L. G., Dhe-Paganon, S., Dimov, S., Dombrovski, L., Finerty, P., Jr., Flodin, S., Flores, A., Gräslund, S., Hammerström, M., Herman, M. D., Hong, B. S., Hui, R., Johansson, I., Liu, Y., Nilsson, M., Nedyalkova, L., Nordlund, P., Nyman, T., Min, J., Ouyang, H., Park, H. W., Qi, C., Rabeh, W., Shen, L., Shen, Y., Sukumard, D., Tempel, W., Tong, Y., Tresagues, L., Vedadi, M., Walker, J. R., Weigelt, J., Welin, M., Wu, H., Xiao, T., Zeng, H., and Zhu, H. (2007) *In situ* proteolysis for protein crystallization and structure determination. *Nat. Methods* **4,** 1019–1021
53. Wernimont, A., and Edwards, A. (2009) *In situ* proteolysis to generate crystals for structure determination: an update. *PLoS One* **4,** e5094
54. Pettersen, E. F., Goddard, T. D., Huang, C. C., Couch, G. S., Greenblatt, D. M., Meng, E. C., and Ferrin, T. E. (2004) UCSF Chimera–a visualization system for exploratory research and analysis. *J. Comp. Chem.* **25,** 1605–1612
55. Wang, Y., and Ge, W. (2004) Cloning of zebrafish ovarian P450c17 (CYP17, 17α-hydroxylase/17,20-lyase) and characterization of its expression in gonadal and extra-gonadal tissues. *Gen. Comp. Endocrinol.* **135,** 241–249
56. Chen, C. F., Wen, H. S., Wang, Z. P., He, F., Zhang, J. R., Chen, X. Y., Jin, G. X., Shi, B., Shi, D., Yang, Y. P., Li, J. F., Qi, B. X., and Li, N. (2010) Cloning and expression of P450c17-I (17α-hydroxylase/17,20-lyase) in brain and ovary during gonad development in *Cynoglossus semilaevis*. *Fish Physiol. Biochem.* **36,** 1001–1012
57. Akhtar, M., Corina, D. L., Miller, S. L., Shyadehi, A. Z., and Wright, J. N. (1994) Incorporation of label from $^{18}O_2$ into acetate during side-chain cleavage catalysed by cytochrome $P450_{17\alpha}$ (17α-hydroxylase-17,20-lyase). *J. Chem. Soc. Perkin Trans.* **1,** 263–267
58. Lee-Robichaud, P., Shyadehi, A. Z., Wright, J. N., Akhtar, M. E., and Akhtar, M. (1995) Mechanistic kinship between hydroxylation and desaturation reactions: acyl-carbon bond cleavage promoted by pig and human CYP17 (P-$450_{17\alpha}$; 17α-hydroxylase-17,20-lyase). *Biochemistry* **34,** 14104–14113
59. Estrada, D. F., Skinner, A. L., Laurence, J. S., and Scott, E. E. (2014) Human cytochrome P450 17A1 conformational selection: modulation by ligand and cytochrome b_5. *J. Biol. Chem.* **289,** 14310–14320
60. Flück, C. E., Miller, W. L., and Auchus, R. J. (2003) The 17,20-lyase activity of cytochrome P450c17 from human fetal testis favors the Δ^5 steroidogenic pathway. *J. Clin. Endocrinol. Metab.* **88,** 3762–3766
61. Bell-Parikh, L. C., and Guengerich, F. P. (1999) Kinetics of cytochrome P450 2E1-catalyzed oxidation of ethanol to acetic acid via acetaldehyde.

J. Biol. Chem. **274,** 23833–23840
62. Chowdhury, G., Calcutt, M. W., and Guengerich, F. P. (2010) Oxidation of *N*-nitrosoalkylamines by human cytochrome P450 2A6: sequential oxidation to aldehydes and carboxylic acids and analysis of reaction steps. *J. Biol. Chem.* **285,** 8031–8044
63. Chowdhury, G., Calcutt, M. W., Nagy, L. D., and Guengerich, F. P. (2012) Oxidation of methyl and ethyl nitrosamines by cytochrome P450 2E1 and 2B1. *Biochemistry* **51,** 9995–10007
64. Guengerich, F. P., Sohl, C. D., and Chowdhury, G. (2011) Multi-step oxidations catalyzed by cytochrome P450 enzymes: Processive *vs*. distributive kinetics and the issue of carbonyl oxidation in chemical mechanisms. *Arch. Biochem. Biophys.* **507,** 126–134
65. Hanson, K. L., VandenBrink, B. M., Babu, K. N., Allen, K. E., Nelson, W. L., and Kunze, K. L. (2010) Sequential metabolism of secondary alkyl amines to metabolic-intermediate complexes: opposing roles for the secondary hydroxylamine and primary amine metabolites of desipramine, (*S*)-fluoxetine, and *N*-desmethyl diltiazem. *Drug Metab. Dispos.* **38,** 963–972
66. Isin, E. M., and Guengerich, F. P. (2007) Complex reactions catalyzed by cytochrome P450 enzymes. *Biochim. Biophys. Acta* **1770,** 314–329
67. Johnson, K. A. (2003) in *Kinetic Analysis of Macromolecules: A Practical Approach* (Johnson, K. A., ed) pp. 1–18, Oxford University Press, Oxford, UK
68. Northrop, D. B. (1982) Deuterium and tritium kinetic isotope effects on initial rates. *Methods Enzymol.* **87,** 607–625
69. Walsh, C. (1979) *Enzymatic Reaction Mechanisms,* pp. 33–35, W. H. Freeman, & Co., San Francisco, CA
70. Yamaoka, M., Hara, T., Araki, H., Kaku, T., Hitaka, T., Tasaka, A., and Kusaka, M. (2013) Effect of an investigational CYP17A1 inhibitor, orteronel (TAK-700), on estrogen- and corticoid-synthesis pathways in hypophysectomized female rats and on the serum estradiol levels in female cynomolgus monkeys. *J. Steroid Biochem. Mol. Biol.* **138,** 298–306
71. Miller, W. L., Geller, D. H., and Auchus, R. J. (1998) The molecular basis of isolated 17,20 lyase deficiency. *Endocr. Res.* **24,** 817–825
72. Geller, D. H., Auchus, R. J., and Miller, W. L. (1999) P450c17 mutations R347H and R358Q selectively disrupt 17,20-lyase activity by disrupting interactions with P450 oxidoreductase and cytochrome b_5. *Mol. Endocrinol.* **13,** 167–175
73. Peng, H. M., Liu, J., Forsberg, S. E., Tran, H. T., Anderson, S. M., and Auchus, R. J. (2014) Catalytically relevant electrostatic interactions of cytochrome P450c17 (CYP17A1) and cytochrome b_5. *J. Biol. Chem.* **289,** 33838–33849
74. Zhu, J., and DeLuca, H. F. (2012) Vitamin D 25-hydroxylase—Four decades of searching, are we there yet? *Arch. Biochem. Biophys.* **523,** 30–36
75. Shimshoni, J. A., Roberts, A. G., Scian, M., Topletz, A. R., Blankert, S. A., Halpert, J. R., Nelson, W. L., and Isoherranen, N. (2012) Stereoselective formation and metabolism of 4-hydroxyretinoic acid enantiomers by cytochrome P450 enzymes. *J. Biol. Chem.* **287,** 42223–42232
76. He, X., Cryle, M. J., De Voss, J. J., and de Montellano, P. R. (2005) Calibration of the channel that determines the ω-hydroxylation regiospecificity of cytochrome P450 4A1: Catalytic oxidation of 12-halododecanoic acids. *J. Biol. Chem.* **280,** 22697–22705
77. Kagawa, N., and Waterman, M. R. (1995) in *Cytochrome P450: Structure, Mechanism, and Biochemistry* (Ortiz de Montellano, P. R., ed) 2nd Ed., pp. 419–442, Kluwer Academic/Plenum Press, New York

Enzymology:

Structural and Kinetic Basis of Steroid 17α,20-Lyase Activity in Teleost Fish Cytochrome P450 17A1 and Its Absence in Cytochrome P450 17A2

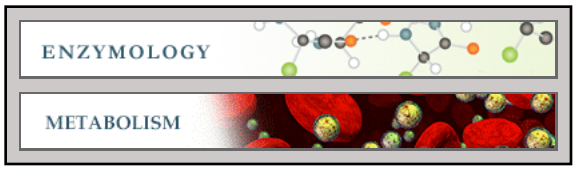

Pradeep S. Pallan, Leslie D. Nagy, Li Lei, Eric Gonzalez, Valerie M. Kramlinger, Caleigh M. Azumaya, Zdzislaw Wawrzak, Michael R. Waterman, F. Peter Guengerich and Martin Egli

J. Biol. Chem. 2015, 290:3248-3268.
doi: 10.1074/jbc.M114.627265 originally published online December 22, 2014